

Vetoing all the Higgs imposters in $H \rightarrow \ell^- \ell^+ Z$

Seong Youl Choi^{a*}, Jaehoon Jeong^{b†}, and Dong Woo Kang^{a‡}

^a*Laboratory for Symmetry and Structure of the Universe, Department of Physics,
Jeonbuk National University, Jeonju 54896, Korea*

^b*School of Physics, Korea Institute for Advanced Study, Seoul 02455, Korea*

Abstract

We develop an effective and methodical algorithm for the construction of general covariant four-point $H\ell\ell Z$ vertices, accommodating leptons $\ell = e, \mu$, and designed to handle a boson H of any integer spin, not merely confined to spins up to 2. While our numerical analysis assumes the H -boson mass to be $m_H = 125$ GeV, the analytical framework we propose is versatile, enabling the examination of various mass as well as spin scenarios. These meticulously devised general covariant four-point $H\ell\ell Z$ vertices are pivotal in vetoing all the imposters of the Standard Model Higgs boson holding the spin-0 and even-parity quantum numbers, especially in one of its primary decay channels, the three-body decay process $H \rightarrow \ell^- \ell^+ Z$, observable at the Large Hadron Collider. Our innovative strategy encompasses the analysis of all the effectively allowed scenarios, extending beyond the limitations of previous investigations on the Higgs spin and parity determinations in the decay $H \rightarrow \ell^- \ell^+ Z$. Based on the significantly expanded scheme, we demonstrate that the Higgs boson imposter of any spin and parity can be definitively vetoed by leveraging threshold effects and angular correlations, even though achieving such conclusive results in practical and exhaustive analyses necessitates high event rates.

*sychoi@jbnu.ac.kr

†jeong229@kias.re.kr

‡dongwookang@jbnu.ac.kr

1 Introduction

The last missing piece of the beautiful tapestry of the Standard Model (SM) [1–4] of particle physics has been filled by the discovery [5, 6] of a Higgs boson consistent with SM predictions at the Large Hadron Collider (LHC). As an authoritative historical review on the SM, we refer to the work [7] by Steven Weinberg, one of the SM founders. Nevertheless, the theory of electroweak (EW) and strong interactions is strongly suggested to be a mere effective theory, underlying a more fundamental theoretical framework, due to various unresolved conceptual issues and unexplained experimental observations [8].

At present, in the absence of definitive and direct discoveries of new physics beyond the SM (BSM), we are confronting a revived period characterized by precision-enhanced measurements and data-driven analyses. While the conventional model-building approach has significantly influenced the strategies for experimental measurements and designs in the quest for new physics over the past fifty years, we are now compelled to rely on a multitude of data-driven precise measurements. This approach is intended to facilitate the exploration of a more fundamental understanding of physics in a model-independent manner, both directly and indirectly. Recently, there has been increasing focus on these model-independent effective methods [9–14], leading to intensified efforts in developing tailored (data-driven) analytical approaches, as evidenced, for example, by the formation of the international seminar series called All Things EFT [15].

The development and evolution of the SM over more than five decades are anchored on two fundamental conceptual foundations. One pillar is the local gauge symmetry of the combined group $SU(3)_C \times SU(2)_L \times U(1)_Y$, governing the strong and unified electroweak interactions. The other pillar is the spontaneous breakdown of the EW symmetry $SU(2)_L \times U(1)_Y$ to the electromagnetic (EM) gauge symmetry $U(1)_{EM}$, triggered by a non-zero vacuum expectation value (vev) of the neutral component of a single Higgs doublet field. This mechanism, first proposed in three seminal works in the year of 1964 [16–18], gives rise to a physical quantum fluctuation of the Higgs doublet field around the vacuum, manifesting as the massive SM Higgs boson announcing the occurrence of the spontaneous breaking of SM electroweak gauge symmetry. It holds specific spin s_H , parity P , and charge-conjugation C quantum numbers:

$$s_H[PC] = 0[++] . \tag{1.1}$$

These attributes are intrinsic to the interactions of the Higgs boson with EW gauge bosons, gluons, photons, and fermions, ensuring conservation of C , P , and CP symmetries [19–21]. To solidify the foundations of the SM, it is crucial to ascertain the spin and parity of the discovered particle with more enhanced certainty, alongside precise measurements and determinations of its interactions with itself and all the SM particles across diverse production and decay channels at the LHC [8, 22–25] and upcoming lepton and hadron colliders [26, 27].

Previous research on the systematic analysis of spin and parity quantum numbers has been extensively worked out in decays such as Z^*Z [28–44], $Z\gamma$ [45–48], and $\gamma\gamma$ decays [49–53], and CP -violating decays [54–58]. These analyses have explored diverse production channels like gluon and vector boson fusion [59–61], Higgs-strahlung and associated Higgs-vector production [62–64]. Nevertheless, additional challenges persist in accurately establishing the spin and parity of the SM Higgs boson [65]. One crucial challenge arises due to limitations in the theoretical frameworks used in previous analyses, which do not comprehensively cover all potential scenarios.

In particular, one part of the past analyses that aimed to identify the spin and parity of the SM Higgs boson via the 3-body decay $H \rightarrow \ell^- \ell^+ Z$ with $\ell = e, \mu$ have relied on a two-step cascade process involving an intermediate virtual Z^* exchange, followed by a leptonic SM Z decay $Z^* \rightarrow \ell^- \ell^+$, in the consideration of the H boson of any integer spin [28–48]. The other part of them has been worked out by considering the process $H \rightarrow \ell^- \ell^+ Z$ occurring via the contact as well as all cascade-channel interactions mainly for the spinless H boson [66–70]. In order to ensure a complete and unambiguous determination of the Higgs spin and parity, it is essential to consider a significantly broader and more general scope, including the general 4-point $H\ell\ell Z$ vertex depicted with a black square in Fig. 1 that represents all potential interactions, encompassing not only the specific two-step cascade process but also additional scenarios involving all permissible channel processes and four-point contact interactions among the four particles, H , ℓ^\pm , and Z , with the H boson of any integer spin. Building upon this substantially expanded framework, we undertake a model-independent and thorough analysis to eliminate all potential Higgs imposters via the decay $H \rightarrow \ell^- \ell^+ Z$, where $\ell = e, \mu$. This approach contributes to a more refined determination of the spin and parity properties of the Standard Model Higgs boson.

As the initial step, we develop an efficient and systematic algorithm for constructing general covariant four-point $H\ell\ell Z$ vertices with $\ell = e, \mu$ for a particle H of any integer spin of which the value does not have to be restricted up to two. Although the H mass is numerically set to $m_H = 125$ GeV [8], our method allows for flexibility in handling different mass values. These carefully constructed general covariant four-point $H\ell\ell Z$ vertices play a crucial role in systematically identifying the spin and parity of the SM Higgs boson through its prime Higgs decay channel, the three-body process $H \rightarrow \ell^- \ell^+ Z$, where $\ell = e, \mu$, at the LHC. We emphasize again that this novel approach surpasses previous analytic platforms for simulation and experimental studies on Higgs spin and parity determination [6, 28–39, 41–45].

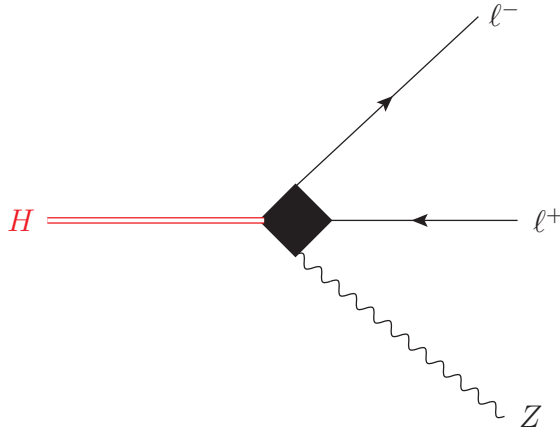


Figure 1: *Diagrammatic description of the four-point $H\ell\ell Z$ vertex the decay process $H \rightarrow \ell^- \ell^+ Z$ for a massive H of any integer spin. In the SM, the particle H can be identified to be the SM Higgs boson with its definite discrete spacetime quantum numbers and well-measured mass $m_H = 125$ GeV. The lepton ℓ is assumed to be e or μ with its mass ignored.*

By leveraging the one-to-one correspondence between the helicity formalism and the covariant

formulation, we construct the general covariant four-point $H\ell\ell Z$ vertices to describe the 3-body decay of the H boson with any integer spin s_H

$$H(s_H, m_H) \rightarrow \ell^-(1/2, m_\ell) + \ell^+(1/2, m_\ell) + Z(1, m_Z), \quad (1.2)$$

in the H rest frame where $\{s_H, 1/2, 1\}$ and $\{m_H, m_\ell, m_Z\}$ are the spins and masses of the particles, $\{H, \ell^\mp, Z\}$, respectively. The methodology for constructing these vertices is a logical and challenging extension of the algorithm used in prior works to build general three-point vertices, as detailed in a sequence of publications [71–73]. The kinematic configuration of the 3-body decay process in the H rest frame is depicted in Fig. 2, where p_H , k_1 , k_2 and k_Z denote the four-momenta for the H boson, two leptons ℓ^\mp and the Z boson, respectively, and λ_H , $\sigma_{1,2}$ and λ_Z denote the H , ℓ^\mp and Z helicities, respectively. The momentum direction of the $\ell^-\ell^+$ system is taken to be along the positive z -axis, while the Z -boson momentum direction is set to be along the negative z -axis.

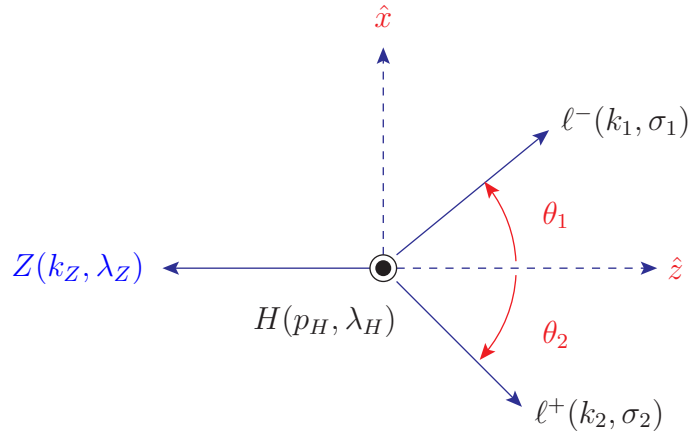


Figure 2: Kinematic configuration of the three-body decay $H(p_H, \lambda_H) \rightarrow \ell^-(k_1, \sigma_1) + \ell^+(k_2, \sigma_2) + Z(k_Z, \lambda_Z)$ in the rest frame of the H boson. Here, p_H , k_1 , k_2 and k_Z are the H , ℓ^- , ℓ^+ and Z four-momenta, while λ_H , σ_1 , σ_2 and λ_Z are their helicities, respectively. θ_1 and θ_2 are the polar angles of the ℓ^- and ℓ^+ momentum directions with respect to the direction opposite to the Z momentum direction, which is set to be the positive z -axis. The decay plane is defined to be the xz plane without any loss of generality, as it will become clear after taking into account the on-shell Z boson decay into a fermion-antifermion pair.

Including the leptonic decays of the on-shell Z boson $Z \rightarrow f\bar{f}$ with $f = e$ and μ , the clean final 4-lepton channels allow us to isolate the signal of the 3-body H decay from the background effectively and to construct the kinematical configuration completely with good precision. While the dominant decay mode for the Higgs mass of 125 GeV is the $b\bar{b}$ channel, the Z^*Z mode with one virtual Z^* boson below the threshold for two real Z bosons is one of the sub-leading channels next to the W^*W channel [74, 75]. We show that the $\ell^-\ell^+$ invariant-mass distributions and various angular correlations in the 3-body decay of the H boson allow for a clear determination of the spin and parity of the SM Higgs boson. This determination remains feasible in such a significantly enlarged scenario that encompasses the general $H\ell\ell Z$ interaction with the H boson with any integer spin s_H , although

conducting practical and comprehensive analyses require high event rates.

The paper is organized as follows. In Sec. 2, we work out the kinematics of the on-shell Z boson and two charged leptons ℓ^\mp in detail, derive two chirality-conserving (CC) $\ell\ell$ vector currents in the massless limit with $m_\ell = 0$ and introduce the general form of integer-spin wave functions expressed as a linear combination of products of spin-1 polarization vectors coupled with the appropriate Clebsch-Gordon coefficients in the H rest frame. All of them play an essential role in constructing the general structure of the covariant 4-point $H\ell\ell Z$ vertices. In Sec. 3 we define and construct all the basic HZ and $\ell\ell$ helicity-specific operators by investigating the decays of a spin-1 particle into two spin-1 massive particles and two spin-1/2 massless particles, respectively. Following the construction of the five fundamental HZ operators and the two essential $\ell\ell$ operators that give rise to the CC lepton vector currents in Sec. 3, we meticulously outline an effective and methodical algorithm for constructing all the helicity-specific covariant $H\ell\ell Z$ vertices in Sec. 4. This development stands as the pivotal outcome of our current study. Section 5 describes all the key characteristics of the invariant mass distribution and angular correlations specific to the SM Higgs boson. After describing the characteristic features of the SM Higgs boson, we demonstrate in Sec. 6 that any scenario of a H imposter with any integer spin or/and odd parity can be ruled out unambiguously through the effective cooperation of the invariant mass distribution and angular correlations. We emphasize that unlike most previous studies, our comprehensive studies include all the allowed 4-point $H\ell\ell Z$ processes, in addition to the standard two-step processes, $H \rightarrow Z^*Z \rightarrow \ell^-\ell^+Z$. Section 7 summarizes several key findings and concludes with a definitive and persuasive statement on a more refined identification of the spin and parity of the Standard Model Higgs through its primary H decay mode. In addition, several analytic formulas to be utilized for evaluating all the helicity amplitudes are collected in Appendix A and a set of integral functions to be used for deriving all the invariant-mass and polar- and azimuthal-angle correlations are listed in Appendix B.

2 Kinematics and wave functions

To systematically develop our algorithm for constructing general covariant four-point $H\ell\ell Z$ vertices and calculating all relevant decay amplitudes and correlations, it is imperative to utilize various kinematic quantities and wave functions. These elements are fundamental in determining the vertex structure. Section 2 is devoted to listing them collectively.

As the electron and muon masses, $m_e = 5.1 \times 10^{-3}$ GeV and $m_\mu = 1.06 \times 10^{-1}$ GeV, are significantly smaller than the scale $v = 246$ GeV of spontaneous electroweak symmetry breaking (EWSB) [8], it is justifiable and generally safe to disregard the masses of light leptons and concentrate solely on the CC interactions from a conceptual standpoint and practical perspective. This approach is valid since the chirality-violating (CV) couplings typically scale with the tiny lepton masses.¹ Then, the $\ell^-\ell^+$ bi-linear term for $\ell = e, \mu$ is assumed to be given by the CC right/left-handed vector current defined by²

$$L_\pm^\mu = \bar{u}(k_1, \pm\frac{1}{2}) \gamma^\mu P_\pm v(k_2, \mp\frac{1}{2}) = -\sqrt{2}im_\star \hat{l}_\pm \quad \text{with} \quad P_\pm = \frac{1 \pm \gamma_5}{2}, \quad (2.1)$$

¹The couplings of the H boson to light leptons and all other effects proportional to $m_{e,\mu}/m_H$ are ignored.

²It is straightforward to include the CV $\ell^-\ell^+$ scalar currents, although not considered in the present work.

with $k = k_1 + k_2$ and $m_\star = \sqrt{k^2}$ is the $\ell^- \ell^+$ invariant mass. Here, the normalized space-like four vectors \hat{l}_\pm satisfy the following orthonormal relations in the limit with $m_\ell = 0$

$$\hat{l}_+ \cdot \hat{l}_+^* = \hat{l}_- \cdot \hat{l}_-^* = -1, \quad \hat{l}_+ \cdot \hat{l}_-^* = \hat{l}_- \cdot \hat{l}_+^* = 0, \quad (2.2)$$

valid in any reference frame.

For the sake of notation, we introduce the following dimensionless kinematic quantities

$$\omega_{\star,Z} = m_{\star,Z}/m_H, \quad \eta^\pm = \sqrt{1 - (\omega_\star \pm \omega_Z)^2}, \quad \kappa = \eta^+ \eta^-, \quad e_{\star,Z} = 1 \pm (\omega_\star^2 - \omega_Z^2), \quad (2.3)$$

which enable us to parameterize the H , ℓ^- , ℓ^+ , and Z four-momenta as

$$k = k_1 + k_2 = p_H - k_Z = m_\star \hat{k}, \quad l = k_1 - k_2 = m_\star \hat{l}, \quad (2.4)$$

$$p_H = k + k_Z = m_H \hat{p}, \quad q = k - k_Z = m_H (\omega_\star^2 - \omega_Z^2) \hat{p} + m_H \kappa \hat{r}, \quad (2.5)$$

in terms of four normalized momenta, \hat{p} , \hat{k} , \hat{l} and \hat{r} , satisfying the normalization conditions, $\hat{p}^2 = \hat{k}^2 = 1$ and $\hat{l}^2 = \hat{r}^2 = -1$. The normalized momenta, \hat{p} and \hat{r} , are simply given by

$$\hat{p} = (1, 0, 0, 0), \quad \hat{r} = (0, 0, 0, 1), \quad (2.6)$$

in the H rest frame with the kinematic configuration in Fig. 2. The normalized momenta, \hat{k} and \hat{l} , and two polar angles, θ_1 and θ_2 , are given by

$$\hat{k} = (\gamma_\star, 0, 0, \gamma_\star \beta_\star), \quad \hat{l} = (\gamma_\star \beta_\star \cos \theta, \sin \theta, 0, \gamma_\star \cos \theta), \quad (2.7)$$

$$\cos \theta_1 = \frac{\beta_\star + \cos \theta}{1 + \beta_\star \cos \theta}, \quad \cos \theta_2 = \frac{\beta_\star - \cos \theta}{1 - \beta_\star \cos \theta}, \quad (2.8)$$

and the space-like normalized vectors \hat{l}_\pm in Eq. (2.1), are orthogonal to both \hat{k} and \hat{l} , and written as

$$\hat{l}_\pm = \pm \frac{1}{\sqrt{2}} (\gamma_\star \beta_\star \sin \theta, -\cos \theta, \pm i, \gamma_\star \sin \theta), \quad (2.9)$$

in terms of the angle θ denoting the polar angle of the lepton ℓ^- with respect to the positive z axis in the rest frame of the $\ell^- \ell^+$ system. The two boost parameters, γ_\star and β_\star , describing the Lorentz transformation of the $\ell^- \ell^+$ system from the CM frame to the H rest frame and the other two boost parameters, γ_Z and β_Z , describing that of the on-shell Z boson from the rest frame to the H rest frame are

$$\gamma_\star = \frac{e_\star}{2\omega_\star}, \quad \beta_\star = \frac{\kappa}{e_\star}; \quad \gamma_Z = \frac{e_Z}{2\omega_Z}, \quad \beta_Z = \frac{\kappa}{e_Z}, \quad (2.10)$$

in the coordinate system defined in Fig. 2. It is noteworthy that the normalized momenta, \hat{p} and \hat{k} , are time-like but the normalized momenta \hat{r} , \hat{l} , and \hat{l}_\pm , are space-like. The invariant products, $\hat{p} \cdot \hat{r} = \hat{k} \cdot \hat{l} = 0$, are vanishing in any reference frame, while the invariant products, $\hat{l} \cdot \hat{p}$ and $\hat{l} \cdot \hat{r}$ are $\gamma_\star \beta_\star \cos \theta$ and $\gamma_\star \cos \theta$, respectively, in the $\ell^- \ell^+$ CM frame.

The wave function of a spin-0 particle is simply 1, which is independent of its mass and momentum. On the other hand, for a non-zero integer spin s , the wave function of an incoming massive boson

with its momentum p and helicity λ is given by a wave tensor defined as a linear combination of products of s spin-1 polarization vectors with appropriate Clebsh-Gordon coefficients by [76–81]

$$\epsilon^{\mu_1 \cdots \mu_s}(p, \lambda) = \sqrt{\frac{2^s (s + \lambda)! (s - \lambda)!}{(2s)!}} \sum_{\{\tau_i\}=\pm 1, 0} \delta_{\tau_1 + \cdots + \tau_s, \lambda} \prod_{j=1}^s \frac{\epsilon^{\mu_j}(k, \tau_j)}{\sqrt{2}^{|\tau_j|}}, \quad (2.11)$$

with the abbreviation $\{\tau_i\} = \tau_1, \dots, \tau_s$. The totally symmetric, traceless, and divergence-free wave function (2.11) enables us to construct all the related interaction vertices efficiently as will be demonstrated later. We note in passing that if the integer-spin particle is massless, the wave tensor has only two maximal-magnitude helicities of $\lambda = \pm s$ and its form is given by a direct product of s spin-1 wave vectors, each of which carries the same helicity of ± 1 . The transverse and longitudinal-polarization vectors of a massive spin-1 particle read

$$\epsilon(p, \pm 1) = \frac{1}{\sqrt{2}} (0, \mp \hat{\theta} - i \hat{\phi}), \quad \epsilon(p, 0) = \frac{1}{m} (|\vec{p}|, E \hat{n}), \quad (2.12)$$

in the helicity basis with the polarization axis along the normalized momentum direction $\hat{n} = (\sin \theta \cos \phi, \sin \theta \sin \phi, \cos \theta)$, forming an orthonormal basis together with two unit vectors $\hat{\theta} = (\cos \theta \cos \phi, \cos \theta \sin \phi, -\sin \theta)$ and $\hat{\phi} = (-\sin \phi, \cos \phi, 0)$.

In the kinematic configuration of Fig. 2 where the H boson is at rest with its 4-momentum $p_H = (1, 0, 0, 0)$, the polarization axis of the H boson can be freely chosen so that it will be set to be the positive z -axis for any explicit analytic evaluation in the following. Then, the incoming polarization vectors of the H boson are given by

$$\epsilon_H(p_H, \pm 1) = \frac{1}{\sqrt{2}} (0, \mp 1, -i, 0), \quad \epsilon_H(p_H, 0) = (0, 0, 0, 1). \quad (2.13)$$

On the other hand, the Z polarization vectors in its helicity basis with the polarization axis along the negative z -axis are written as

$$\epsilon_Z(k_Z, \pm 1) = \frac{1}{\sqrt{2}} (0, \mp 1, i, 0), \quad \epsilon_Z(k_Z, 0) = \frac{1}{2\omega_Z} (\kappa, 0, 0, -e_Z), \quad (2.14)$$

in the helicity formalism with the Wick convention [82–87] slightly modified from the so-called Jacob-Wick (JW) convention [88].

3 Constructing helicity-specific operators

In this section, we define and construct all the basic HZ and $\ell\ell$ helicity-specific operators necessary for weaving the general 4-point $H\ell\ell Z$ vertices systematically and compactly.

The initial step is to derive all five Lorentz-covariant basic HZ helicity-specific operators by investigating the two-body decay $H \rightarrow XZ$ of a spin-1 massive particle H into two spin-1 massive particles X and Z . Each of these operators generates a nonzero decay amplitude solely for a specific configuration $[\lambda_H, \lambda_Z]$ of the H and Z helicities in the H rest frame when coupled to the wave

functions [71–73]. Their expressions and roles in transitions originating from the $[0, 0]$ point in the HZ helicity space are articulated as follows:

$$U_{\beta\alpha}^0 \hat{p}_{\star\mu} = \hat{p}_{Z\beta} \hat{r}_{H\alpha} \hat{p}_{\star\mu} \quad \rightarrow \quad [\lambda_H, \lambda_Z] = [0, 0], \quad (3.1)$$

$$U_{\mu\alpha}^{\pm} \hat{p}_{Z\beta} = \frac{1}{2} [g_{\perp\mu\alpha} \pm i \langle \mu\alpha \hat{p} \hat{r} \rangle] \hat{p}_{Z\beta} \quad \rightarrow \quad [\lambda_H, \lambda_Z] = [\pm 1, 0], \quad (3.2)$$

$$U_{\mu\beta}^{\pm} \hat{r}_{H\alpha} = \frac{1}{2} [g_{\perp\mu\beta} \pm i \langle \mu\beta \hat{p} \hat{r} \rangle] \hat{r}_{H\alpha} \quad \rightarrow \quad [\lambda_H, \lambda_Z] = [0, \pm 1]. \quad (3.3)$$

where the four-vector indices, α , μ , and β , are associated with the spin-1 H , X , and Z bosons, respectively. These are defined in terms of two normalized momenta, \hat{p} and \hat{r} , in Eq. (2.5), and three re-scaled momenta: $\hat{r}_{H\alpha} = \kappa \hat{r}_\alpha$, $\hat{p}_{\star\mu} = 2\omega_{\star} \hat{p}_\mu$, and $\hat{p}_{Z\beta} = 2\omega_Z \hat{p}_\beta$. The re-scaled momentum $\hat{r}_{H\alpha} = \kappa \hat{r}_\alpha$ is intentionally introduced because the normalized space-like four-vector \hat{r} is always accompanied with the kinematic factor κ as shown in Eq. (2.5).

For conceptual clarity and compact notation, we introduce the square-bracket notations as $U_{\alpha\mu}^{\pm} = [U_H^{\pm}]_{\alpha\mu}$, $U_{\beta\mu}^{\mp} = [U_Z^{\pm}]_{\beta\mu}$ and $U_{\alpha\beta}^0 = [U_{HZ}^0]_{\alpha\beta} = \hat{r}_{H\alpha} \hat{p}_{Z\beta}$. The implications of the four basic HZ operators, U_H^{\pm} and U_Z^{\pm} , governing the horizontal and vertical one-step helicity transitions in the HZ helicity space can be illustrated in Fig. 3. The two orthogonal tensors $g_{\perp\mu\nu}$ and $\langle \mu\nu \hat{p} \hat{r} \rangle$ are defined by

$$g_{\perp\mu\nu} = g_{\mu\nu} - \hat{p}_\mu \hat{p}_\nu + \hat{r}_\mu \hat{r}_\nu, \quad (3.4)$$

$$\langle \mu\nu \hat{p} \hat{r} \rangle = \varepsilon_{\mu\nu\rho\sigma} \hat{p}^\rho \hat{r}^\sigma, \quad (3.5)$$

in terms of the totally antisymmetric Levi-Civita tensor $\varepsilon_{\mu\nu\rho\sigma}$ with the convention of $\varepsilon_{0123} = +1$. Contracting two basic HZ operators, U_H^{\pm} and U_Z^{\mp} , lead to two composite transition operators governing the right-down and left-up diagonal one-step transitions in the HZ helicity space as

$$U_{\beta\alpha}^{\pm} = g^{\mu\nu} U_{\mu\beta}^{\mp} U_{\nu\alpha}^{\pm} = \frac{1}{2} [g_{\perp\beta\alpha} \pm i \langle \beta\alpha \hat{p} \hat{r} \rangle] \quad \rightarrow \quad [\lambda_H, \lambda_Z] = [\pm 1, \mp 1], \quad (3.6)$$

each of which yields a nonzero decay amplitude only for the configuration $[\lambda_H, \lambda_Z] = [+1, -1]$ or $[-1, +1]$ of the H and Z helicities.

In the second phase of our approach, we introduce the covariant CC basic $\ell\ell$ operators W_{\pm} re-scaled by the H mass m_H , leading to the dimensionless amplitude of a two-body decay $X \rightarrow \ell^- \ell^+$ for a spin-1 particle X :

$$W_{\pm}^{\mu} = \frac{i}{\sqrt{2}m_H} \gamma^{\mu} P_{\pm}, \quad (3.7)$$

with the chiral projection operators $P_{\pm} = (1 \pm \gamma_5)/2$. The imaginary number $i = \sqrt{-1}$ is factored out for removing it emerging in the helicity amplitude computation according to the Wick convention.

In the third step, given the complexity arising from the involvement of many 4-vector indices, especially in the context of high-spin states, we adopt a set of compact square-bracket notations. These notations are designed to succinctly represent the diverse array of indices encountered in the expression of general covariant vertices. Accompanying these notations, we also provide their respective component expressions to ensure clarity and facilitate the understanding of their roles

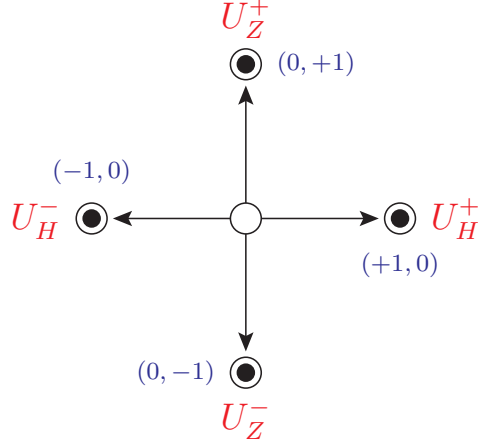


Figure 3: Diagrammatic description of the four bosonic U_H^\pm and U_Z^\pm operators. In components, $[U_H^\pm]_{\alpha\mu} = U_{\alpha\mu}^\pm$ and $[U_Z^\pm]_{\beta\mu} = U_{\beta\mu}^\pm$, which are defined simply by the same set of two basic operators U^\pm . The detailed expressions are listed in Eqs. (3.2) and (3.3).

within the general vertices as

$$[\hat{p}_\star] \rightarrow \hat{p}_{\star\mu} = 2\omega_\star \hat{p}_\mu, \quad (3.8)$$

$$[\hat{p}_Z] \rightarrow \hat{p}_{Z\beta} = 2\omega_Z \hat{p}_\beta, \quad (3.9)$$

$$[\hat{r}_H] \rightarrow \hat{r}_{H\alpha} = \kappa \hat{r}_\alpha, \quad (3.10)$$

$$[U_{HZ}^\pm] \rightarrow U_{\beta\alpha}^\pm, \quad (3.11)$$

$$[\hat{r}_H]^n \rightarrow \hat{r}_{H\alpha_1} \cdots \hat{r}_{H\alpha_n} = \kappa^n \hat{r}_{\alpha_1} \cdots \hat{r}_{\alpha_n}, \quad (3.12)$$

$$[U_H^\pm]^n \rightarrow U_{\mu_1\alpha_1}^\pm \cdots U_{\mu_n\alpha_n}^\pm, \quad (3.13)$$

$$[U_Z^\pm] \rightarrow U_{\mu\beta}^\pm. \quad (3.14)$$

For any operator or re-scaled momentum, its zeroth power term with $n = 0$ is set to 1 for convenience. Without loss of generality, any arrangement of the α four-vector indices is ultimately absorbed into the symmetric nature of the H wave tensors, rendering all the permutations of these indices effectively identical. Additionally, it's worth noting that the re-scaled momenta, \hat{p}_\star and \hat{p}_Z vanish when their corresponding masses, m_\star and m_Z , are set to zero such that only the operators corresponding to the maximal-magnitude helicity values survive in the massless limit, thereby rendering their theoretical treatment automatic and accurate.

4 Weaving helicity-specific covariant four-point vertices

We are now ready to express the helicity amplitude of the decay process $H \rightarrow \ell^- \ell^+ Z$ in the covariant formulation, which can be written in a factorized form as

$$\mathcal{M}_{\lambda_H; \sigma, \lambda_Z}^{[H \rightarrow \ell\ell Z]}(\theta) = c_{\lambda_H; \sigma, \lambda_Z}^{[H\ell\ell Z]} \left\{ \epsilon_{\lambda_Z}^{\star\beta}(k_Z, \lambda_Z) [\mathcal{H}_{[\lambda_H, \lambda_Z]}^{j_0[HZ]}]_{\bar{\alpha}, \beta}^{\bar{\mu}} \epsilon_H^{\bar{\alpha}}(p_H, \lambda_H) \right\} \left\{ \bar{u}(k_1, \frac{\sigma}{2}) [\mathcal{H}_{[\sigma]}^{j_0[\ell\ell]}]_{\bar{\mu}} v(k_2, -\frac{\sigma}{2}) \right\}, \quad (4.1)$$

in the H rest frame with $j_0 = \max(|\lambda_H + \lambda_Z|, |\sigma|)$, where $\bar{\alpha} = \alpha_1 \cdots \alpha_{s_H}$ is the collection of 4-vector indices of the spin- s_H wave tensor of the H boson, β is the four-vector index of the spin-1 Z and $\bar{\mu} = \mu_1 \cdots \mu_{j_0}$. Note that j_0 is no less than the unity because of $|\sigma| = 1$ in the CC case. All the 4-momenta and helicities are denoted in Fig. 2. Contracting the general $\ell\ell$ helicity-specific operator $\mathcal{H}_{[\sigma]}^{j_0[\ell\ell]}$ with the general HZ helicity-specific operator $\mathcal{H}_{[\lambda_H, \lambda_Z]}^{j_0[HZ]}$ results in a four-point $H\ell\ell Z$ vertex operator in an operator form as

$$[\mathcal{H}_{[\lambda_H; \sigma, \lambda_Z]}^{j_0[H\ell\ell Z]}] = c_{\lambda_H; \sigma, \lambda_Z}^{[H\ell\ell Z]} [\mathcal{H}_{[\lambda_H, \lambda_Z]}^{j_0[HZ]}] \cdot [\mathcal{H}_{[\sigma]}^{j_0[\ell\ell]}], \quad (4.2)$$

with a form factor $c_{\lambda_H; \sigma, \lambda_Z}^{[H\ell\ell Z]}$ for the specific helicity configurations $[\lambda_H; \sigma, \lambda_Z]$. Each of the form factors depends generally on the invariant products of momenta, all of which can be expressed by combining $m_\star = \sqrt{k^2}$ and $\hat{l} \cdot \hat{p}_\star = \kappa \cos \theta$. It implies that any parity-odd combination of the form factors is proportional to at least the single power of $\kappa \cos \theta$.

Let us show how to assemble the general form of the covariant four-point vertex in Eq. (4.2) by use of the general $\ell\ell$ - and HZ -helicity-specific operators, step by step. First, each of the general $\ell\ell$ operators must be constructed by one basic $\ell\ell$ operator W_\pm and a multiple product of the normalized four-vector \hat{l} as

$$\mathcal{H}_{[\sigma]}^{j_0[\ell\ell]\bar{\mu}} = \omega_\star^{j_0-1} W_\sigma^{\mu_1} \hat{l}^{\mu_2} \cdots \hat{l}^{\mu_{j_0}} \quad \text{with} \quad W_\sigma^{\mu_1} = \frac{i}{\sqrt{2}m_H} \gamma^{\mu_1} P_\sigma \quad \text{and} \quad j_0 \geq 1, \quad (4.3)$$

with the chiral projection operator $P_\sigma = (1 + \sigma\gamma_5)/2$, and the abbreviation $\bar{\mu} = \mu_1\mu_2 \cdots \mu_{j_0}$. For the sake of efficient evaluation and analysis, we introduce the contraction between the basic $\ell\ell$ operators $W_\sigma^{\mu_1}$ and the massless spinors, $u(\ell^-)$ and $v(\ell^+)$, so as to read straightforwardly the $\ell\ell$ vertex part in the decay amplitude as

$$\bar{u}(k_1, \frac{\sigma}{2}) [\mathcal{H}_{[\sigma]}^{j_0[\ell\ell]}] \bar{\mu} v(k_2, \frac{\sigma}{2}) = \omega_\star^{j_0} \hat{l}_\sigma^{\mu_1} \hat{l}^{\mu_2} \cdots \hat{l}^{\mu_{j_0}}, \quad (4.4)$$

where the j_0 -th power term of $\omega_\star^{j_0}$ is introduced to properly take into account the kinematical properties of the original chiral leptonic vector currents L_\pm in Eq. (2.1) and the momentum difference $l = k_1 - k_2 = m_H \omega_\star \hat{l}$ varying with $\omega_\star = m_\star/m_H$.

Certainly, the simplest case for the decay process $H \rightarrow \ell^- \ell^+ Z$ is when $s_H = 0$, i.e. H is a spin-0 scalar like the SM Higgs boson with no helicity at all. The Z -boson spin is $s_Z = 1$ so that the value of $j_0 = \max(|\lambda_Z|, |\sigma|)$ is also 1. In this case, the $\ell\ell$ operators are $[\mathcal{H}_{[\sigma]}^{1[\ell\ell]}]^\mu = W_\sigma^\mu$ and the three independent HZ -helicity-specific operators are

$$[\mathcal{H}_{[\bullet, \pm 1]}^{1[HZ]}]_{\beta\mu} = U_{\beta\mu}^\pm = U_{\mu\beta}^\mp \quad \text{and} \quad [\mathcal{H}_{[\bullet, 0]}^{1[HZ]}]_{\beta\mu} = U_{\beta\mu}^0 = \hat{p}_{\star\mu} \hat{p}_{Z\beta} = 4\omega_\star \omega_Z \hat{p}_\mu \hat{p}_\beta, \quad (4.5)$$

of which the corresponding three helicity points are displaced in the left panel of Fig. 4. The bullet notation \bullet in Eq. (4.5) is used to indicate the spinless nature of the H boson with $s_H = 0$. Consequently, combining the operators, $[\mathcal{H}_{[\sigma]}^{1[\ell\ell]}]$ and $[\mathcal{H}_{[\bullet, \lambda_Z]}^{1[HZ]}]$, over the μ index, we have six ($6 = 2 \times 3$) independent terms with the Lorentz-invariant m_\star - and $\hat{l} \cdot \hat{p}_\star$ -dependent coefficients. Note that $\hat{l} \cdot \hat{p}_\star = \kappa \cos \theta$ in the $e^- e^+$ CM frame in Fig. 2.

When the spin of the massive H boson is $s_H = 1$, there are nine HZ operators for each of two $\ell\ell$ operators, as described in the right frame of Fig. 4 and listed in Tab. 1. Consequently, there are in

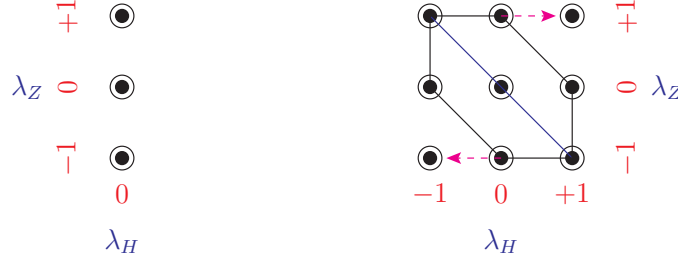


Figure 4: Diagrammatic representation of the lattice structure of the helicity space for both the H and Z particles in scenarios involving a spin-0 H boson (on the left) and a spin-1 H boson (on the right). For illustration, three (nine) points are displayed for the spin-0 (spin-1) case. In the right diagram, the seven points connected through solid lines correspond to the total spin $j_0 = 1$ mode, while the two points connected by the magenta dashed arrows correspond to the total spin $j_0 = 2$ mode. The value of j_0 is one plus the total number of dashed lines required to reach the point from each reference point.

s_H	j_0	(λ_H, λ_Z)	$[\mathcal{H}_{[\sigma]}^{j_0[\ell\ell]}]$	$[\mathcal{H}_{[\lambda_H, \lambda_Z]}^{j_0[HZ]}]$	#
1	1	$(\pm 1, \mp 1), (0, 0)$	$W_{\sigma}^{\mu_1}$	$U_{\beta\alpha}^{\pm} \hat{p}_{\star\mu_1}, \hat{r}_{H\alpha} \hat{p}_{\star\mu_1} \hat{p}_{Z\beta}$	3
		$(\pm 1, 0), (0, \pm 1)$		$U_{\mu_1\alpha}^{\pm} \hat{p}_{Z\beta}, U_{\mu_1\beta}^{\pm} \hat{r}_{H\alpha}$	4
	2	$(\pm 1, \pm 1)$	$\omega_{\star} W_{\sigma}^{\mu_1} \hat{l}^{\mu_2}$	$U_{\mu_1\alpha}^{\pm} U_{\mu_2\beta}^{\pm}$	2

Table 1: The table of two $\ell\ell$ -helicity-specific operators with $\sigma = \pm 1$ and nine HZ -helicity-specific operators with a massive spin-1 particle H classified according to the values of j_0 and each (λ_H, λ_Z) helicity combination for the spin-1 H .

total eighteen independent terms with proper Lorentz-invariant m_{\star} - and $\hat{l} \cdot \hat{p}_{\star}$ -dependent coefficients. The invariant product $\hat{l} \cdot \hat{p}_{\star} = \kappa \cos \theta$ is always accompanied by a kinematical factor κ .

When the spin of the H boson is $s_H = 2$, there are fifteen HZ -helicity-specific operators for each of two $\ell\ell$ -helicity-specific operators, as listed in Tab. 2. Its pictorial description can be inferred from the diagram in Fig. 5, restricting $|\lambda_H| \leq 2$. Consequently, there are in total thirty independent terms with proper Lorentz-invariant m_{\star} - and $\hat{l} \cdot \hat{p}_{\star}$ -dependent coefficients.

Finally, if the H spin is $s_H \geq 3$, there are in total $3(2s_H + 1)$ HZ operators for each of two $\ell\ell$ operators as shown in Fig. 5. The $j_0 = 1$ category has nine independent HZ terms. In addition, for each Z helicity, $\lambda_Z = \pm 1, 0$ there are $2(s_H - 1)$ independent HZ for all the $j_0 > 1$ categories. Summing them, we have $3 \times 2(s_H - 1) + 9 = 3(2s_H + 1)$ as expected. Consequently, there are in total $6(2s_H + 1)$ independent terms with Lorentz-invariant coefficients dependent only on m_{\star} and $\hat{l} \cdot \hat{p}_{\star}$.

For a given j_0 , the general CC $\ell\ell$ operators are nothing but $[\mathcal{H}_{[\sigma]}^{j_0[\ell\ell]}]$ of which the expression was

s_H	j_0	(λ_H, λ_Z)	$[\mathcal{H}_{[\sigma]}^{j_0[\ell\ell]}]$	$[\mathcal{H}_{[\lambda_H, \lambda_Z]}^{j_0[HZ]}]$	#
2	1	$(\pm 1, \mp 1), (0, 0)$	$W_\sigma^{\mu_1}$	$U_{\alpha_1\beta}^\pm \hat{r}_{H\alpha_2} \hat{p}_{\star\mu_1}, \hat{r}_{H\alpha_1} \hat{r}_{H\alpha_2} \hat{p}_{\star\mu_1} \hat{p}_{Z\beta}$	3
		$(\pm 2, \mp 1), (\pm 1, 0), (0, \pm 1)$		$U_{\mu_1\alpha_1}^\pm U_{\beta\alpha_2}^\pm, U_{\mu_1\alpha_1}^\pm \hat{r}_{H\alpha_2} \hat{p}_{Z\beta}, U_{\mu_1\beta}^\pm \hat{r}_{H\alpha_1} \hat{r}_{H\alpha_2}$	6
	2	$(\pm 1, \pm 1)$	$\omega_\star W_\sigma^{\mu_1} \hat{l}^{\mu_2}$	$U_{\mu_1\alpha_1}^\pm U_{\mu_2\beta}^\pm \hat{r}_{H\alpha_2}$	2
		$(\pm 2, 0)$		$U_{\mu_1\alpha_1}^\pm U_{\mu_2\alpha_2}^\pm \hat{p}_{Z\beta}$	2
		3	$(\pm 2, \pm 1)$	$\omega_\star^2 W_\sigma^{\mu_1} \hat{l}^{\mu_2} \hat{l}^{\mu_3}$	$U_{\mu_1\alpha_1}^\pm U_{\mu_2\alpha_2}^\pm U_{\mu_3\beta}^\pm$

Table 2: The table of two $\ell\ell$ -helicity-specific operators with $\sigma = \pm 1$ and fifteen HZ -helicity-specific operators with a spin-2 massive particle H , classified according to three allowed values of $j_0 = 1, 2, 3$ and each available (λ_H, λ_Z) helicity combination.

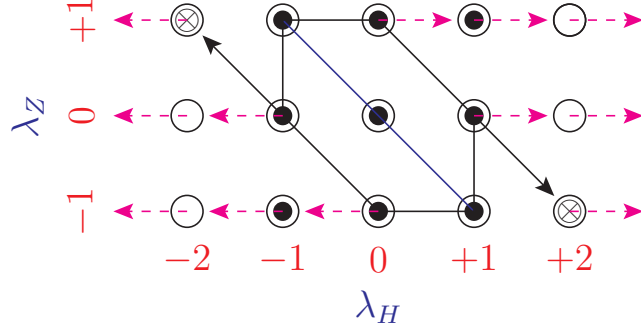


Figure 5: Diagrammatic description of the lattice structure of the H and Z helicity space. For illustration, fifteen points are displayed for the case up to $s_H = 2$. The nine points connected through solid lines correspond to the $j_0 = 1$ mode, while the points connected by magenta dashed arrows correspond to the $j_0 > 1$ modes. The value of j_0 is one plus the total number of dashed arrows required to reach the point from each starting reference point. For example, the j_0 value of the point $(\lambda_H, \lambda_Z) = (\pm 2, \pm 1)$ is $3 = |\pm 2 \pm 1|$ as it involves two dashed lines.

given previously in Eq. (4.3). They can be cast into the following operator form

$$[\mathcal{H}_{[\sigma]}^{j_0[\ell\ell]}] = \omega_\star^{j_0-1} [W_\sigma][\hat{l}]^{j_0-1} \Rightarrow \mathcal{H}_{[\sigma]}^{j_0[\ell\ell]\bar{\mu}} = \omega_\star^{j_0-1} W_\sigma^{\mu_1} \hat{l}^{\mu_2} \dots \hat{l}^{\mu_{j_0}}, \quad (4.6)$$

with $\bar{\mu} = \mu_1 \dots \mu_{j_0}$. We emphasize again that the $\omega_\star^{j_0-1}$ term is introduced to take into account the dependence of the momentum difference $l = k_1 - k_2$ on the varying $\ell^- \ell^+$ invariant mass m_\star .

Note that all the HZ -helicity-specific operators related to the two-body decay of the H boson include only two independent normalized momenta, \hat{p} and \hat{r} . The HZ -helicity-specific operators are

categorized into six parts as

$$[\mathcal{H}_{[0,0]}^{j_0[HZ]}] = [\hat{r}_H]^{s_H} [\hat{p}_\star][\hat{p}_Z] \quad \text{with } j_0 = 1, \quad (4.7)$$

$$[\mathcal{H}_{[0,\pm 1]}^{j_0[HZ]}] = [\hat{r}_H]^{s_H} [U_Z^\pm] \quad \text{with } j_0 = 1, \quad (4.8)$$

$$[\mathcal{H}_{[\pm 1,\mp 1]}^{j_0[HZ]}] = [\hat{r}_H]^{s_H-1} [U_{HZ}^\pm][\hat{p}_\star] \quad \text{with } j_0 = 1, \quad (4.9)$$

$$[\mathcal{H}_{[\pm n,0]}^{j_0[HZ]}] = [\hat{r}_H]^{s_H-n} [U_H^\pm]^n [\hat{p}_Z] \quad \text{with } j_0 = n, \quad (4.10)$$

$$[\mathcal{H}_{[\pm \tilde{n},\mp 1]}^{j_0[HZ]}] = [\hat{r}_H]^{s_H-\tilde{n}} [U_H^\pm]^{\tilde{n}-1} [U_{HZ}^\pm] \quad \text{with } j_0 = \tilde{n} - 1, \quad (4.11)$$

$$[\mathcal{H}_{[\pm n,\pm 1]}^{j_0[HZ]}] = [\hat{r}_H]^{s_H-n} [U_H^\pm]^n [U_Z^\pm] \quad \text{with } j_0 = n + 1, \quad (4.12)$$

where $n = 1, \dots, s_H$ and $\tilde{n} = 2, \dots, s_H$. In total we can compute the total number of independent HZ operators by summing the degrees of freedom of all the categories as

$$n[s_H] = 1 + 2 + 2 + 2s_H + 2(s_H - 1) + 2s_H = 3(2s_H + 1), \quad (4.13)$$

as expected. The first factor of 3 in the last expression reflects that the Z boson is a spin-1 massive particle with $3 = 2 \times 1 + 1$ degrees of freedom.

Equivalently, the CC helicity amplitude (4.1) of the decay process $H \rightarrow \ell^- \ell^+ Z$ in the rest frame of the H boson can be generally decomposed in the helicity formalism [82–87] into one dynamical part \mathcal{T} and a pure angular part denoted by a Wigner d function as

$$\mathcal{M}_{\lambda_H;\sigma,\lambda_Z}^{[H \rightarrow \ell\ell Z]}(\theta) = \mathcal{T}_{\lambda_H;\sigma,\lambda_Z}^{[H\ell\ell Z]}(m_\star, \kappa \cos \theta) d_{\lambda_H+\lambda_Z,\sigma}^{j_0}(\theta), \quad (4.14)$$

in terms of the polar angle θ defining the ℓ^- momentum direction of the $\ell^- \ell^+$ CM system with respect to the positive z -axis, where $j_0 = \max(|\lambda_H + \lambda_Z|, |\sigma|)$ is the minimal value of the angular momenta of the $\ell^- \ell^+$ CM system for the fixed helicity configuration.³ The explicit form of the Wigner d function can be found in several standard angular-momentum textbooks, for instance, in Ref. [89]. For convenience, a comprehensive set of analytic formulas useful for systematically and efficiently calculating the helicity amplitudes is provided in Appendix A.

It is worthwhile to emphasize that the reduced helicity amplitudes $\mathcal{T}_{\lambda_H;\sigma,\lambda_Z}^{[H\ell\ell Z]}$ depend at most on the $\ell^- \ell^+$ invariant mass m_\star and the cosine of the polar-angle, $\cos \theta$, accompanied without exception by κ in the combination of $\kappa \cos \theta$. If the form factors are for any contact vertices, they are independent of the angular variable. In general, their behaviors rely on the three Lorentz-invariant Mandelstam variables [90], which are defined to be

$$s = (p_H - k_Z)^2 = (k_1 + k_2)^2 = m_\star^2, \quad (4.15)$$

$$t = (p_H - k_1)^2 = (k_Z + k_2)^2 = (m_H^2 + m_Z^2 - m_\star^2 - m_H^2 \kappa \cos \theta)/2, \quad (4.16)$$

$$u = (p_H - k_2)^2 = (k_Z + k_1)^2 = (m_H^2 + m_Z^2 - m_\star^2 + m_H^2 \kappa \cos \theta)/2, \quad (4.17)$$

with their explicit form derived in the H rest frame. As argued previously, the Mandelstam variables take $s = (m_H - m_Z)^2$ and $t = u = m_H m_Z$ at the threshold with $m_\star = m_H - m_Z$, being independent

³ $d_{\lambda_H+\lambda_Z,\sigma}^j(\theta)$ with $j > j_0$ is a simple product of $d_{\lambda_H+\lambda_Z,\sigma}^{j_0}(\theta)$ and a $(j - j_0)$ -th order polynomial of $\cos \theta$.

of the polar angle θ indicating that the Z boson and the $\ell^-\ell^+$ system are produced at rest.

The specific form of the Wigner d function in Eq. (4.14) is guaranteed by the characteristic feature that any helicity is Lorentz invariant with trivial Wick helicity rotation in the massless limit so that the decay helicity amplitude in the H rest frame is identical to that in the $\ell^-\ell^+$ CM frame [85–87]. The Wigner d function takes the following explicit forms [89]:

$$d_{\pm j_0, \sigma}^{j_0}(\theta) = (-1)^{j_0-1} \sqrt{\frac{(2j_0)!}{(j_0+1)!(j_0-1)!}} \left(\frac{\sin \theta}{2}\right)^{j_0-1} d_{\pm 1, \sigma}^1(\theta), \quad (4.18)$$

for $j_0 = |\lambda_H + \lambda_Z| \geq 1$ with $d_{\pm 1, \sigma}^1(\theta) = (1 + \sigma \cos \theta)/2$ and it is necessary to introduce one additional Wigner d function

$$d_{0, \sigma}^1(\theta) = \frac{\sigma}{\sqrt{2}} \sin \theta, \quad (4.19)$$

for $j_0 = |\sigma| = 1$ when $\lambda_H + \lambda_Z = 0$.

As mentioned before, the H polarization states will be averaged out eventually in evaluating every physical observable under consideration so that the H polarization axis can be set to be opposite to the flight direction of the Z boson, as described in Fig. 2, for much more efficient analytic calculation. Nevertheless, if required, the H decay process can be connected straightforwardly with its production mechanism by explicitly specifying the H polarization axis with its own polar and azimuthal angles, θ_H and ϕ_H as well as an azimuthal angle ϕ for denoting the coordinate-independent geometrical orientation of the $\ell^-\ell^+$ system with respect to the polarization axis of the H boson. In this case, the three-body decay helicity amplitudes of the H boson is written as

$$\mathcal{M}_{\lambda_H; \sigma, \lambda_Z}^{[H \rightarrow \ell \ell Z]}(\theta_H, \phi_H; \theta, \phi) = \sum_{\lambda'_H = -s_H}^{s_H} D_{\lambda'_H, \lambda_H}^{s_H*}(\pi + \phi, \theta_H, \phi_H) \mathcal{M}_{\lambda'_H; \sigma, \lambda_Z}^{[H \rightarrow \ell \ell Z]}(\theta), \quad (4.20)$$

with the simplified decay helicity amplitude $\mathcal{M}_{\lambda'_H; \sigma, \lambda_Z}^{[H \rightarrow \ell \ell Z]}$ in Eq. (4.14), where the rotation matrix elements $D_{\lambda'_H, \lambda_H}^{s_H*}$ are defined to be

$$D_{\lambda'_H, \lambda_H}^{s_H*}(\pi + \phi, \theta_H, \phi_H) = e^{i\lambda'_H(\pi + \phi)} d_{\lambda'_H, \lambda_H}^{s_H}(\theta_H) e^{i\lambda_H \phi_H}, \quad (4.21)$$

which satisfies the orthogonality property for the solid-angle integration on the unit sphere as

$$\int d\phi d\Omega_H D_{\lambda'_H, \lambda_H}^{s_H*}(\pi + \phi, \theta_H, \phi_H) D_{\lambda''_H, \lambda_H}^{s_H}(\pi + \phi, \theta_H, \phi_H) = \frac{8\pi^2}{2s_H + 1} \delta_{\lambda'_H, \lambda''_H}, \quad (4.22)$$

with the differential solid-angle measure $d\Omega_H = \sin \theta_H d\theta_H d\phi_H$.

We emphasize that the reduced helicity amplitudes $\mathcal{T}_{\lambda_H; \sigma, \lambda_Z}^{[H \ell \ell Z]}(m_\star, \kappa \cos \theta)$ do not require the introduction of any cut-off scale Λ , probably indicating the energy scale of a new physics. Our theoretical description operates beyond the limitations of low-energy regimes by allowing the form factors $c^{[H \ell \ell Z]}$ in Eq. (4.1) to be functions of particle momenta without restriction to low powers. One notable common feature is the polar-angle θ independence of all the form factors at the threshold with $m_\star = m_H - m_Z$ rendering the value of κ zero. In this regard, the pure angular component denoted by the Wigner d function may be regarded as the minimal angular distribution for any given helicity combination.

5 Characteristic decay patterns of the SM Higgs boson

As mentioned before, the spin s_H , parity P and charge conjugation C quantum numbers of the SM Higgs boson are necessarily $s_H[PC] = 0[++]$ by the construction of the SM with the EW gauge symmetry hidden or spontaneously broken [2, 3]. Therefore, establishing the basic structure of the SM requires identifying the spin and parity of the Higgs state as well as other characteristic features through as many available processes as possible at the ongoing LHC and future high-energy lepton and hadron collider experiments.

One of the prime Higgs decay modes for its spin and parity identification, which actually has played a crucial role in discovering the Higgs boson [5, 6], is the 3-body decay process of the SM Higgs boson $H \rightarrow \ell^- \ell^+ Z$ proceeding through the production $H \rightarrow Z^* Z$ of a virtual boson Z^* and its sequential two-body leptonic decay $Z^* \rightarrow \ell^- \ell^+$ with $\ell = e, \mu$:

$$H \rightarrow Z^* + Z \rightarrow \ell^- \ell^+ + Z, \quad (5.1)$$

where the virtual Z^* can be treated as an on-shell spin-1 particle of varying mass $m_\star = \sqrt{k^2}$ in the CC limit of neglecting the lepton masses. In the kinematic configuration in Fig. 2, the polarization vectors of the off-shell Z^* boson, whose the polarization axis is set to be along the positive z -axis, are given by

$$\epsilon_\star(k, \pm 1) = \frac{1}{\sqrt{2}}(0, \mp 1, -i, 0), \quad \epsilon_\star(k, 0) = \frac{1}{2\omega_\star}(\kappa, 0, 0, e_\star), \quad (5.2)$$

so that the helicity amplitudes of the three-body decay $H \rightarrow \ell^- \ell^+ Z$ can be decomposed into one Z^* production part and one Z^* decay part connected by a virtual Z^* propagator as

$$\mathcal{M}[H \rightarrow Z^* Z \rightarrow \ell^- \ell^+] = \frac{1}{m_\star^2 - m_Z^2 + im_Z \Gamma_Z} \mathcal{P}[H \rightarrow Z^* Z] \mathcal{D}[Z^* \rightarrow \ell^- \ell^+], \quad (5.3)$$

where the helicity amplitudes for the two-body decay $H \rightarrow Z^* Z$ and the other two-body decay $Z^* \rightarrow \ell^- \ell^+$ explicitly read

$$\mathcal{P}[H \rightarrow Z^*(\lambda_\star) Z(\lambda_Z)] = g_Z m_Z [\epsilon^*(k, \lambda_\star) \cdot \epsilon^*(k_Z, \lambda_Z)] = g_Z m_Z P_{\lambda_Z, \lambda_Z}, \delta_{\lambda_\star, \lambda_Z} \quad (5.4)$$

$$\mathcal{D}[Z^*(\lambda_\star) \rightarrow \ell^-(\frac{\sigma}{2}) \ell^+(\frac{-\sigma}{2})] = i\sqrt{2} g_Z m_\star [v_\sigma \hat{l}_\sigma \cdot \epsilon(k, \lambda_\star)] = -i\sqrt{2} g_Z m_\star v_\sigma^\ell D_{\lambda_\star, \sigma}, \quad (5.5)$$

with $g_Z = e/c_W s_W$, $v_+ = s_W^2$ and $v_- = s_W^2 - 1/2$ in terms of the proton electric charge e and the cosine and sine, $c_W = \cos \theta_W$ and $s_W = \sin \theta_W$, of the weak mixing angle θ_W . The helicity values λ_\star and λ_Z of the off-shell Z^* and on-shell Z bosons are ± 1 or 0 . Note that the imaginary number i is explicitly taken out to set the normalized chiral lepton current \hat{l}_σ to be a pure spin-1 polarization vector in the Wick convention.

The metric tensor $g_{\beta\mu}$ of even normality $n_H \equiv (-1)^{s_H} P = +$ defines the pure scalar coupling of the SM Higgs boson to two $Z^{(*)}$ bosons. This coupling is generated characteristically through EWSB and can be effectively decomposed in terms of fundamental HZ operators and re-scaled momenta as

$$\langle Z_\mu^* Z_\beta | H \rangle_{\text{SM}} = g_Z m_Z g_{\mu\beta} \Rightarrow g_{\mu\beta} = U_{\mu\beta}^+ + U_{\mu\beta}^- + \frac{1 - \omega_\star^2 - \omega_Z^2}{2\omega_\star \omega_Z \kappa^2} \hat{p}_{\star\mu} \hat{p}_{Z\beta}. \quad (5.6)$$

The decomposition (5.6) enables us to derive the helicity amplitudes P_{λ_*, λ_Z} straightforwardly, of which the three non-zero Z^* production amplitudes read

$$P_{\pm 1, \pm 1} = -1, \quad P_{0,0} = \frac{1 - \omega_Z^2 - \omega_*^2}{2\omega_Z\omega_*} = \frac{m_H^2 - m_Z^2 - m_*^2}{2m_Z m_*}. \quad (5.7)$$

On the other hand, the helicity amplitudes of the two-body decay $Z^* \rightarrow \ell^- \ell^+$ can be cast into the pure kinematical angular-dependent form:

$$D_{\pm 1, \sigma} = \frac{1 \pm \sigma \cos \theta}{2} = d_{\pm 1, \sigma}^1(\theta), \quad D_{0, \sigma} = \frac{\sigma}{\sqrt{2}} \sin \theta = d_{0, \sigma}^1(\theta), \quad (5.8)$$

apart from the chiral vector coupling v_σ with $\sigma = \pm 1$, in terms of the polar angle θ denoting the ℓ^- flight direction in the $\ell^- \ell^+$ CM frame. Note that the $Z^* \rightarrow \ell^- \ell^+$ decay amplitudes are invariant under the boost along the Z^* polarization axis, as guaranteed from the feature that the helicity of a massless particle is a Lorentz-invariant quantity.

Based on the explicit forms of the decay helicity amplitudes, we extract and summarize the essential points for measuring the spin and parity of the SM Higgs boson. Firstly, the partial decay width of the process $H \rightarrow Z^* Z$ is given in the SM by

$$\Gamma(H \rightarrow Z^* Z) = \frac{3G_F^2 m_Z^4}{8\pi^3} \delta_Z m_H R(\omega_Z), \quad (5.9)$$

where $\delta_Z = 7/12 - 10s_W^2/9 + 40s_W^4/27$ and the ω_Z -dependent function $R(\omega_Z)$ is decomposed as

$$R(\omega_Z) = (1 - 4\omega_Z^2 + 12\omega_Z^4)A_0(\omega_Z) - 2(1 - 6\omega_Z^2)A_1(\omega_Z) + A_2(\omega_Z), \quad (5.10)$$

of which the expression is given in the limit of neglecting the Z -boson width Γ_Z by [30, 62, 74, 75, 91]

$$R(\omega_Z) = \frac{3(1 - 8\omega_Z^2 + 20\omega_Z^4)}{2\sqrt{4\omega_Z^2 - 1}} \cos^{-1} \left(\frac{3\omega_Z^2 - 1}{2\omega_Z^3} \right) - \frac{1 - \omega_Z^2}{4\omega_Z^2} (2 - 13\omega_Z^2 + 47\omega_Z^4) - \frac{3}{2} (1 - 6\omega_Z^2 + 4\omega_Z^4) \log \omega_Z. \quad (5.11)$$

The integral-form definition of the ω_Z -dependent functions $A_n(\omega_Z)$ and their explicit forms from $n = 0$ to 5 in the limit of neglecting the Z -boson width can be found in Appendix B. The invariant-mass spectrum m_* of the off-shell Z^* boson exhibits a rapid rise as m_* increases, followed by a sharp decline near the kinematic limit where $m_* = m_H - m_Z$, signifying zero momentum of the off-shell Z^* and on-shell Z bosons in the final state. Its precise expression is given by

$$\frac{d\Gamma_H}{dm_*} = \frac{3G_F^2 m_Z^4 \delta_Z}{8\pi^3 m_H} \cdot \frac{m_*(12m_*^2 m_Z^2 + m_H^4 \kappa^2)}{(m_*^2 - m_Z^2)^2 + m_Z^2 \Gamma_Z^2} \kappa = \frac{\Gamma_H}{m_H R(\omega_Z)} \frac{\omega_*(12\omega_*^2 \omega_Z^2 + \kappa^2)}{(\omega_*^2 - \omega_Z^2)^2 + \omega_Z^2 \Gamma_Z^2 / m_H^2} \kappa, \quad (5.12)$$

where κ is the magnitude of the Z and Z^* momenta in units of $m_H/2$ in the H rest frame, i.e. $\kappa^2 = [1 - (\omega_Z + \omega_*)^2][(1 - (\omega_Z - \omega_*)^2)]$. The invariant-mass spectrum decreases linearly with κ and therefore steeply with the invariant mass m_* just below the threshold:

$$\frac{d\Gamma_H}{dm_*} \sim \kappa \sim \sqrt{m_H - m_Z - m_*}. \quad (5.13)$$

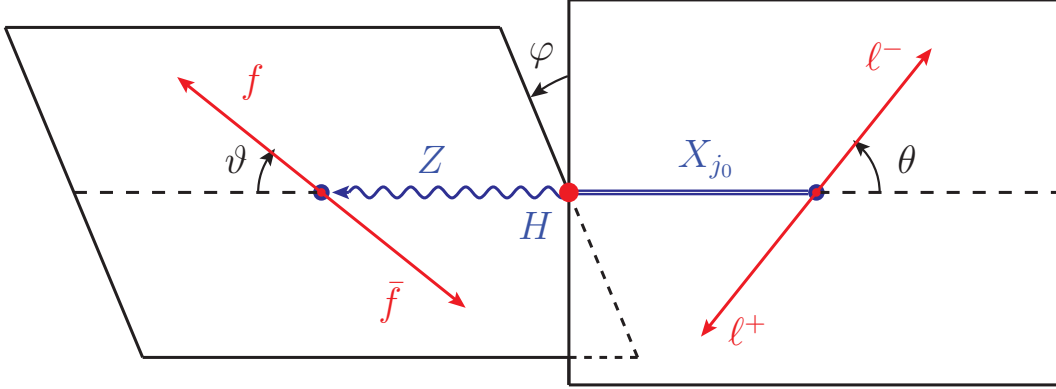


Figure 6: The definition of the polar angles, θ and ϑ , and the azimuthal angle φ for the sequential decay $H \rightarrow \ell^- \ell^+ Z \rightarrow (\ell^- \ell^+) (f \bar{f})$ with $\ell = e, \mu$ and $f = e^-, \mu^-$ in the rest frame of the H particle. The polar angle θ is defined in the rest frame of the $\ell^- \ell^+$ system and the polar angle ϑ of the lepton f with respect to the Z -boson flight direction in the rest frame of the on-shell Z boson. The azimuthal angle φ is the relative angle between two decay planes. The notation X is introduced for denoting the mixed quantum state of the $\ell^- \ell^+$ system collectively. The value of the allowed angular momentum j_0 is fixed to 1 for the intermediate virtual Z^* in the CC limit of massless leptons, but it generally can take a positive integer from 1 up to $s_H + 1$.

This step decrease near the threshold is characteristic of the decay of the SM Higgs boson into two massive vector bosons of which the dimensionless coupling is generated solely through EWSB.

Correlated polar and azimuthal angle distributions give independent and complementary access to spin and parity of the H boson as well. Denoting the two polar angles of the lepton ℓ and the fermion f in the decays $Z^* \rightarrow \ell^- \ell^+$ and $Z \rightarrow f \bar{f}$ in the rest frame of the virtual Z^* and on-shell Z states by θ and ϑ , respectively, and the azimuthal angle between the lepton-pair plane and the fermion-pair plane by φ as depicted in Fig. 6, the correlated distribution in $\cos \theta$ and $\cos \vartheta$ of the off/on-shell Z^* and Z bosons in the SM is predicted to be

$$\frac{d^3 \Gamma_H}{dm_* d \cos \theta d \cos \vartheta} = \frac{d \Gamma_H}{dm_*} \frac{9}{16} \left\{ \frac{4m_*^2 m_Z^2 + m_H^4 \kappa^2}{12m_Z^2 m_*^2 + m_H^4 \kappa^2} \sin^2 \theta \sin^2 \vartheta + \frac{2m_*^2 m_Z^2}{12m_Z^2 m_*^2 + m_H^4 \kappa^2} [(1 + \cos^2 \theta)(1 + \cos^2 \vartheta) + 4\eta_\ell \eta_f \cos \theta \cos \vartheta] \right\}, \quad (5.14)$$

with the invariant-mass distribution in Eq. (5.12), while the corresponding distribution with respect to the azimuthal angle φ is

$$\frac{d^2 \Gamma_H}{dm_* d \varphi} = \frac{d \Gamma_H}{dm_*} \frac{1}{2\pi} \left[1 - \eta_\ell \eta_f \frac{9\pi^2 m_Z m_* (m_H^2 - m_Z^2 - m_*^2)}{12m_Z^2 m_*^2 + m_H^4 \kappa^2} \cos \varphi + \frac{2m_Z^2 m_*^2}{12m_Z^2 m_*^2 + m_H^4 \kappa^2} \cos 2\varphi \right], \quad (5.15)$$

where $\eta_\ell = \eta_f = (v_-^2 - v_+^2)/(v_-^2 + v_+^2)$ is the polarization asymmetry factor of the fermion in the decay processes $Z \rightarrow \ell^- \ell^+$ and $Z \rightarrow f \bar{f}$ with $\ell, f = e, \mu$, and $\gamma_{*,Z}$ and $\beta_{*,Z}$ are the boost factors

and speeds of the off-shell Z^* and on-shell Z bosons in Eq. (2.10), respectively, in the H rest frame. Numerically, the polarization asymmetry factor $\eta_{\ell,f} = 0.237$ for a charged lepton of $f = e, \mu$. After integrating the correlated invariant-mass and polar-angle distribution (5.14) over the invariant mass m_* from 0 to $m_H - m_Z$, we obtain the normalized polar-angle correlation as

$$\frac{d^2 \mathcal{N}_H}{d \cos \theta d \cos \vartheta} = \frac{9}{16} \left\{ \frac{R_L(\omega_Z)}{R(\omega_Z)} \sin^2 \theta \sin^2 \vartheta + \frac{R_T(\omega_Z)}{R(\omega_Z)} \left[\frac{(1 + \cos^2 \theta)(1 + \cos^2 \vartheta)}{4} + \eta_{\ell} \eta_f \cos \theta \cos \vartheta \right] \right\}, \quad (5.16)$$

of which the integral over the polar angle ϑ leads to the normalized single polar-angle distribution

$$\frac{d \mathcal{N}_H}{d \cos \theta} = \frac{3}{4} \left[\frac{R_L(\omega_Z)}{R(\omega_Z)} \sin^2 \theta + \frac{R_T(\omega_Z)}{R(\omega_Z)} \frac{1 + \cos^2 \theta}{2} \right], \quad (5.17)$$

with the ω_Z dependent functions given by

$$R_L(\omega_Z) = (1 - 2\omega_Z^2)^2 A_0(\omega_Z) - 2(1 - 2\omega_Z^2) A_1(\omega_Z) + A_2(\omega_Z), \quad (5.18)$$

$$R_T(\omega_Z) = 8\omega_Z^2 [\omega_Z^2 A_0(\omega_Z) + A_1(\omega_Z)], \quad (5.19)$$

with $R(\omega_Z) = R_L(\omega_Z) + R_T(\omega_Z)$ identical to the expression (5.11). Integrating the correlated distribution (5.15) over the invariant mass yields the azimuthal-angle distribution

$$\frac{d \mathcal{N}_H}{d \varphi} = \frac{1}{2\pi} \left[1 + \eta_{\ell} \eta_f \frac{9\pi^2}{64} \frac{R_1(\omega_Z)}{R(\omega_Z)} \cos \varphi + \frac{R_2(\omega_Z)}{R(\omega_Z)} \cos 2\varphi \right], \quad (5.20)$$

where the explicit expressions of the ω_Z -dependent functions, R_1 and R_2 , can be decomposed as

$$R_1(\omega_Z) = -4\omega_Z [(1 - 2\omega_Z^2) B_0(\omega_Z) - B_1(\omega_Z)], \quad (5.21)$$

$$R_2(\omega_Z) = R_T(\omega_Z)/4, \quad (5.22)$$

where the integral-form definition of the ω_Z -dependent functions A_n , B_n and their explicit forms expressed in terms of three types of elliptic integrals can be found in Appendix B. Quantitatively, for $m_Z = 91 \text{ GeV}$ and $m_H = 125 \text{ GeV}$, $R_L = 0.59R$, $R_T = 0.41R$, $R_1 = -0.64R$ and $R_2 = 0.10R$.

6 Vetoing Higgs imposters

In this section, we investigate step by step how to veto all the Higgs imposters unambiguously through the invariant-mass threshold behavior and 4-lepton polar and azimuthal angle distributions by identifying the features of each Higgs imposter distinct from those of the SM Higgs boson.

6.1 The case with a cascade decay $H \rightarrow Z^* Z \rightarrow \ell^- \ell^+ Z$

First, we consider the case when all the contact terms are negligible and the $\ell^- \ell^+$ final state is generated simply through an off-shell vector boson Z^* fixing the value of j_0 to be 1 in the CC case. In general, a photon-mediated part might be present. However, this contribution can be easily ruled out as its photon propagator part leads to a significantly different invariant-mass distribution from the Z propagator part, especially in the region with a small invariant mass m_* due to the huge

enhancement factor of m_Z^4/m_\star^4 . The helicity amplitude of the decay $H \rightarrow Z_\star Z \rightarrow \ell^- \ell^+ Z$ can be decomposed into two parts as

$$\mathcal{M}_{\lambda_H, \sigma, \lambda_Z}^{[H \rightarrow \ell^- \ell^+ Z]} = 8G_F m_Z^2 \mathcal{T}_{\lambda_\star, \lambda_Z} \frac{m_Z m_\star}{m_\star^2 - m_Z^2 + i m_Z \Gamma_Z} v_\sigma d_{\lambda_\star, \sigma}^1(\theta), \quad (6.1)$$

with the constraint $\lambda_\star = \lambda_H + \lambda_Z = \pm 1, 0$ for the helicity of the off-shell Z^\star boson, $\sigma = \pm 1$, and the chiral vector couplings, v_σ , in the CC case. Here, the reduced helicity amplitudes $\mathcal{T}_{\lambda_\star, \lambda_Z}$ of the two-body decay $H \rightarrow Z^\star Z$ can be re-written apart from a constant coefficient as

$$\mathcal{T}_{\lambda_\star, \lambda_Z} = \epsilon_Z^{\ast\beta}(k_Z, \lambda_Z) \epsilon_\star^{\ast\mu}(k, \lambda_\star) [\mathcal{H}_{[\lambda_H, \lambda_Z]}^{1[HZ]}]_{\bar{\alpha}, \beta, \mu} \epsilon^{\bar{\alpha}}(p_H, \lambda_H), \quad (6.2)$$

in terms of the helicity-specific tensor $[\mathcal{H}_{[\lambda_H, \lambda_Z]}^{1[HZ]}]$ with the constraint $\lambda_\star = \lambda_H + \lambda_Z = \pm 1, 0$ for any value of the H spin, because all the polarization axes of the H , Z_\star and Z bosons are set to be along the z axis. It is noteworthy that any general $HZ^\star Z$ vertex can be expressed effectively as a linear combination of the basic operators $[\mathcal{H}^{1[HZ]}]$, of which the independent number is three (3) for $s_H = 0$, seven (7) for $s_H = 1$ and nine (9) for $s_H \geq 2$ with no more increase of the number of independent terms, as analyzed systematically in Sec. 4.

6.1.1 Fully-correlated CP -invariant distributions

In a CP -invariant theory, the H -boson state can be attributed to a conserved quantum number called normality $n_H = (-1)^{s_H} P$, which links the helicity amplitudes that are connected under parity transformations. If the interactions determining the $HZ^\star Z$ vertex are parity-invariant, the reduced helicity amplitudes are related as,

$$\mathcal{T}_{\lambda_\star, \lambda_Z} = n_H \mathcal{T}_{-\lambda_\star, -\lambda_Z}, \quad (6.3)$$

with the H normality, $n_H = (-1)^{s_H} P$. The fully-combined invariant-mass and angular correlation is decomposed into two parts⁴

$$\frac{d^4 \Gamma_H}{dm_\star d \cos \theta \cos \vartheta d\varphi} \sim \frac{m_\star^3 \kappa}{(m_\star^2 - m_Z^2)^2 + m_Z^2 \Gamma_Z^2} \frac{d^3 \Gamma_H}{d \cos \theta d \cos \vartheta d\varphi}, \quad (6.4)$$

apart from a constant coupling factor, where the full angular correlation part is given by

$$\begin{aligned} \frac{d^3 \Gamma_H}{d \cos \theta d \cos \vartheta d\varphi} &\sim 2 \sin^2 \theta \sin^2 \vartheta |\mathcal{T}_{0,0}|^2 + (1 + \cos^2 \theta)(1 + \cos^2 \vartheta) [|\mathcal{T}_{+1,+1}|^2 + |\mathcal{T}_{+1,-1}|^2] \\ &+ 2(1 + \cos^2 \theta) \sin^2 \vartheta |\mathcal{T}_{+1,0}|^2 + 2 \sin^2 \theta (1 + \cos^2 \vartheta) |\mathcal{T}_{0,+1}|^2 \\ &+ 4 \sin \theta \cos \theta \sin \vartheta \cos \vartheta \cos \varphi \operatorname{Re}(\mathcal{T}_{+1,+1} \mathcal{T}_{0,0}^\ast - \mathcal{T}_{+1,0} \mathcal{T}_{0,-1}^\ast) \\ &+ \sin^2 \theta \sin^2 \vartheta \cos 2\varphi \operatorname{Re}(\mathcal{T}_{+1,+1} \mathcal{T}_{-1,-1}^\ast) \\ &- 4\eta_\ell \sin \theta \sin \vartheta \cos \vartheta \sin \varphi \operatorname{Im}(\mathcal{T}_{+1,+1} \mathcal{T}_{0,0}^\ast - \mathcal{T}_{+1,0} \mathcal{T}_{0,-1}^\ast) \\ &- 4\eta_f \sin \theta \cos \theta \sin \vartheta \sin \varphi \operatorname{Im}(\mathcal{T}_{+1,+1} \mathcal{T}_{0,0}^\ast + \mathcal{T}_{+1,0} \mathcal{T}_{0,-1}^\ast) \\ &+ 4\eta_\ell \eta_f \cos \theta \cos \vartheta [|\mathcal{T}_{+1,+1}|^2 - |\mathcal{T}_{+1,-1}|^2] \\ &+ 4\eta_\ell \eta_f \sin \theta \sin \vartheta \cos \varphi \operatorname{Re}(\mathcal{T}_{+1,+1} \mathcal{T}_{0,0}^\ast + \mathcal{T}_{+1,0} \mathcal{T}_{0,-1}^\ast). \end{aligned} \quad (6.5)$$

⁴Although the case with mixed normality states is not investigated in the present work, we note that it is straightforward to extend our formalism to accommodate the mixed case.

in terms of the reduced helicity amplitudes $\mathcal{T}_{\lambda_*,\lambda_Z}$ describing the two-body decay $H \rightarrow Z^*Z$. Integrating the correlated distribution only over the azimuthal angle φ generates a correlated polar-angle distribution

$$\begin{aligned} \frac{d^2\Gamma_H}{d\cos\theta d\cos\vartheta} &\sim 2\sin^2\theta\sin^2\vartheta|\mathcal{T}_{0,0}|^2 + (1+\cos^2\theta)(1+\cos^2\vartheta)[|\mathcal{T}_{+1,+1}|^2 + |\mathcal{T}_{+1,-1}|^2] \\ &\quad + 2(1+\cos^2\theta)\sin^2\vartheta|\mathcal{T}_{+1,0}|^2 + 2\sin^2\theta(1+\cos^2\vartheta)|\mathcal{T}_{0,+1}|^2 \\ &\quad + 4\eta_\ell\eta_f\cos\theta\cos\vartheta[|\mathcal{T}_{+1,+1}|^2 - |\mathcal{T}_{+1,-1}|^2], \end{aligned} \quad (6.6)$$

while integrating the correlated distribution over the polar and azimuthal angles, ϑ and φ , generates a single polar-angle distribution

$$\frac{d\Gamma_H}{d\cos\theta} \sim \sin^2\theta(|\mathcal{T}_{0,0}|^2 + 2|\mathcal{T}_{0,+1}|^2) + (1+\cos^2\theta)(|\mathcal{T}_{+1,+1}|^2 + |\mathcal{T}_{+1,-1}|^2 + |\mathcal{T}_{+1,0}|^2), \quad (6.7)$$

which is to be combined with Z^* propagator factor as in Eq. (6.4) before being utilized for characterizing the spin and parity of the H boson explicitly in the following. On the other hand, integrating the correlated distribution over the two polar angles, θ and ϑ , generates a single azimuthal-angle distribution

$$\frac{d\Gamma_H}{d\varphi} \sim \sum_{\lambda_*,\lambda_Z} |\mathcal{T}_{\lambda_*,\lambda_Z}|^2 + \frac{9\pi^2}{32}\eta_\ell\eta_f\cos\varphi\text{Re}(\mathcal{T}_{+1,+1}\mathcal{T}_{0,0}^* + \mathcal{T}_{+1,0}\mathcal{T}_{0,-1}^*) + \frac{1}{2}\cos 2\varphi\text{Re}(\mathcal{T}_{+1,+1}\mathcal{T}_{-1,-1}^*), \quad (6.8)$$

which is to be combined with Z^* propagator factor as in Eq. (6.4) for the correlated m_* and φ distribution.

6.1.2 Ruling out all the Higgs imposters

The leading κ dependence of the helicity amplitudes can be determined by counting the number of momenta in each term of the tensor $[\mathcal{H}_{[\lambda_H,\lambda_Z]}^{1[HZ]}]_{\bar{\alpha},\beta,\mu}$. Each re-scaled momentum, which is represented by $\hat{p}_{Z\beta}$ and/or $\hat{r}_{H\alpha}$, contracted with the Z -boson polarization vector or the H -boson polarization tensor will necessarily give zero or one power of κ . Furthermore, the normalized momentum $\hat{p}_{*\mu}$ contracted with the lepton current will give rise to one power of κ due to the transversality of the current. The overall κ dependence of the invariant mass spectrum can be derived from the absolute square of the helicity amplitude multiplied by a single factor κ from the phase space.

- **Spin 0.** If the particle H is an odd-normality pseudo-scalar, i.e. its parity is odd, the HZ^*Z vertex term is given by a parity-odd tensor in any CP-invariant theory which is expressed by a linear combination of the basic HZ operators for the spin-0 H boson in Eq. (4.5) as

$$\frac{1}{m_H^2}\langle\mu\beta pq\rangle = \kappa\langle\mu\beta\hat{p}\hat{r}\rangle = -i\kappa(U_{\mu\beta}^+ - U_{\mu\beta}^-), \quad (6.9)$$

with $p = k + k_Z$ and $q = k - k_Z$, giving rise to $\mathcal{T}_{0,0} = 0$ and non-zero $\mathcal{T}_{+1,+1} = -\mathcal{T}_{-1,-1} \propto i\kappa$ apart from a constant coefficient. Consequently, the invariant mass spectrum decreases in proportion to κ^3 near the kinematical limit and the single polar-angle distribution is simply proportional

to $(1 + \cos^2 \theta)$ with no $\sin^2 \theta$ term. Explicitly, the normalized invariant-mass distribution is given by

$$\frac{d\mathcal{N}_H}{dm_\star} = \frac{m_\star^3 \kappa^2}{\mathcal{P}(\omega_Z) [(m_\star^2 - m_Z^2)^2 + m_Z^2 \Gamma_Z^2]} \kappa, \quad (6.10)$$

with the ω_Z -dependent function \mathcal{P} decomposed as

$$\mathcal{P}(\omega_Z) = \omega_Z^2 (1 - 4\omega_Z^2) A_0(\omega_Z) + (1 - 6\omega_Z^2) A_1(\omega_Z) - (2 - \omega_Z^2) A_2(\omega_Z) + A_3(\omega_Z), \quad (6.11)$$

where the explicit form of the ω_Z -dependent function $A_n(\omega_Z)$ with n from 0 to 5 in the limit of neglecting the Z -boson decay width Γ_Z is listed in Appendix B. The normalized single polar-angle and azimuthal-angle distributions are given simply by

$$\frac{d\mathcal{N}_H}{d \cos \theta} = \frac{3}{8} (1 + \cos^2 \theta) \quad \text{and} \quad \frac{d\mathcal{N}_H}{d\varphi} = \frac{1}{2\pi} \left(1 - \frac{1}{4} \cos 2\varphi \right), \quad (6.12)$$

which are completely independent of both the H and Z -boson masses. Therefore, it is definite that the spin-0 and parity-even SM Higgs boson cannot be imitated by any pseudo-scalar Higgs imposter. For various previous detailed studies on the general scalar H couplings, see for example Refs. [92–97].

- **Spin 1.** Every term in $[\mathcal{H}_{[\lambda_H, \lambda_Z]}^{1[HZ]}]_{\bar{\alpha}, \beta, \mu}$ involves at least one power of momentum. This seems to imply that every helicity amplitude vanishes near the threshold linearly in κ . However, there arises a critical issue that requires a solution by incorporating a suitable factor dependent on the parameter κ . In general, the spin-1 tensor may include an odd-normality term $\langle \alpha \beta \mu_1 \hat{p} \rangle$. This tensor is decomposed effectively into the HZ operators with $s_H = 1$ in Table. 1 as

$$\langle \mu \beta \alpha \hat{p} \rangle = \frac{ie_Z}{2\omega_Z \kappa} (U_{\mu\alpha}^+ - U_{\mu\alpha}^-) \hat{p}_{Z\beta} + \frac{ie_\star}{2\omega_\star \kappa} (U_{\beta\alpha}^+ - U_{\beta\alpha}^-) \hat{p}_{\star\mu} - \frac{i}{\kappa} (U_{\mu\beta}^+ - U_{\mu\beta}^-) \hat{r}_{H\alpha}. \quad (6.13)$$

As a result of this decomposition, we can observe straightforwardly that the helicity amplitudes do not vanish at the threshold, even after the operator is contracted with the H , Z^\star and Z polarization vectors. On the other hand, this decomposition leads to $\mathcal{T}_{0,0} = 0$ so that no $\sin^2 \theta \sin^2 \vartheta$ polar-angle correlation is generated. Instead, it gives rise to the $\sin^2 \theta (1 + \cos^2 \vartheta)$ and $(1 + \cos^2 \theta) \sin^2 \vartheta$ polar-angle correlations, which are not present in the SM. Explicitly, the normalized invariant-mass distribution reads

$$\frac{d\mathcal{N}_H}{dm_\star} = \frac{m_\star [12m_\star^2 m_Z^2 + m_H^2 (m_\star^2 + m_Z^2) \kappa^2]}{m_H^2 \mathcal{K}(\omega_Z) [(m_\star^2 - m_Z^2)^2 + m_Z^2 \Gamma_Z^2]} \kappa, \quad (6.14)$$

where the ω_Z -dependent function \mathcal{K} is given by

$$\mathcal{K}(\omega_Z) = 2\omega_Z^2 (1 + 2\omega_Z^2) A_0(\omega_Z) + (1 + 4\omega_Z^2) A_1(\omega_Z) - 2(1 - \omega_Z^2) A_2(\omega_Z) + A_3(\omega_Z). \quad (6.15)$$

The normalized single polar-angle distribution can be decomposed into two parts as

$$\frac{d\mathcal{N}_H}{d \cos \theta} = \frac{3}{4} \left[\frac{\mathcal{K}_L(\omega_Z)}{\mathcal{K}(\omega_Z)} \sin^2 \theta + \frac{\mathcal{K}_T(\omega_Z)}{\mathcal{K}(\omega_Z)} \frac{(1 + \cos^2 \theta)}{2} \right]. \quad (6.16)$$

The expressions of two ω_Z -dependent functions $\mathcal{K}_{T,L}$ are given by

$$\mathcal{K}_L(\omega_Z) = \omega_Z^2 [A_0(\omega_Z) + 2A_1(\omega_Z) + A_2(\omega_Z)], \quad (6.17)$$

$$\begin{aligned} \mathcal{K}_T(\omega_Z) &= \omega_Z^2 (1 + 4\omega_Z^2) A_0(\omega_Z) + (1 + 2\omega_Z^2) A_1(\omega_Z) \\ &\quad - (2 - \omega_Z^2) A_2(\omega_Z) + A_3(\omega_Z), \end{aligned} \quad (6.18)$$

of which the sum is $\mathcal{K} = \mathcal{K}_L + \mathcal{K}_T$. Numerically, $\mathcal{K}_L = 0.498 \mathcal{K}$ and $\mathcal{K}_T = 0.502 \mathcal{K}$ for $m_Z = 91$ GeV and $m_H = 125$ GeV. And the normalized azimuthal-angle distribution by

$$\frac{d\mathcal{N}_H}{d\varphi} = \frac{1}{2\pi} \left[1 + \frac{9\pi^2}{64} \eta_\ell \eta_f \frac{\mathcal{K}_1(\omega_Z)}{\mathcal{K}(\omega_Z)} \cos \varphi + \frac{\mathcal{K}_2(\omega_Z)}{\mathcal{K}(\omega_Z)} \cos 2\varphi \right], \quad (6.19)$$

where the expressions of two ω_Z -dependent functions $\mathcal{K}_{1,2}$ are

$$\mathcal{K}_1(\omega_Z) = -\omega_Z [B_0(\omega_Z) - B_2(\omega_Z)], \quad (6.20)$$

$$\mathcal{K}_2(\omega_Z) = -\omega_Z^2 [\omega_Z^2 A_0(\omega_Z) + A_1(\omega_Z)]. \quad (6.21)$$

Numerically, $\mathcal{K}_1 = -0.34 \mathcal{K}$ and $\mathcal{K}_2 = -0.06 \mathcal{K}$ for $m_Z = 91$ GeV and $m_H = 125$ GeV. The integral-form definition and integrated expression of each $A_n(\omega_Z)$ with $n = 0$ to 5 and those of each $B_n(\omega_Z)$ from $n = 0$ to 4 are listed in Appendix B.

- **Spin 2.** The general HZ^*Z vertex for the spin-2 H contains a term with no momentum dependence

$$[\mathcal{H}^{1[HZ]}]_{\alpha_1\alpha_2,\mu,\beta} \sim g_{\alpha_1\mu} g_{\alpha_2\beta}, \quad (6.22)$$

generating helicity amplitudes that do not vanish at the threshold. As a concrete spin-2 example, we adopt the interaction vertex of the even-normality first Kaluza-Klein (KK) graviton with a virtual Z^* boson and an on-shell Z boson in the framework of large extra dimensions [98, 99]. Apart from a gauge-fixing term with no physical impact, the covariant HZ^*Z vertex for the spin-2 H is given by

$$\Gamma_{\mu\beta;\alpha_1\alpha_2} = \frac{2}{m_H} [(m_Z^2 + k \cdot k_Z) g_{\mu\alpha_1} g_{\beta\alpha_2} - g_{\mu\alpha_1} k_\beta k_{Z\alpha_2} - g_{\beta\alpha_1} k_{Z\mu} k_{\alpha_2} + g_{\mu\beta} k_{\alpha_1} k_{Z\alpha_2}], \quad (6.23)$$

up to an overall coupling constant, where the indices $\alpha_1\alpha_2$ are for the symmetric and traceless spin-2 wave tensor of the decaying particle H and the indices μ and β are for the virtual Z^* and real Z polarization vectors [100]. The vertex of the spin-2 H imposter can be expressed in terms of the general HZ operators $[\mathcal{H}_{[\lambda_H,\lambda_Z]}^{1[HZ]}]$ in Table. 2 effectively as

$$\begin{aligned} \Gamma_{\mu\beta;\alpha_1\alpha_2} &= m_H \left[e_Z (U_{\mu\alpha_1}^+ U_{\beta\alpha_2}^+ + U_{\mu\alpha_1}^- U_{\beta\alpha_2}^-) + \frac{e_Z - \kappa^2}{2\kappa^2} (U_{\mu\beta}^+ + U_{\mu\beta}^-) \hat{r}_{H\alpha_1} \hat{r}_{H\alpha_2} \right. \\ &\quad - \frac{e_Z^2 - \kappa^2}{2\omega_Z \kappa^2} (U_{\mu\alpha_1}^+ + U_{\mu\alpha_1}^-) \hat{p}_{Z\beta} \hat{r}_{H\alpha_2} + \frac{e_* e_Z - \kappa^2}{2\omega_* \kappa^2} (U_{\beta\alpha_1}^+ + U_{\beta\alpha_1}^-) \hat{p}_{*\mu} \hat{r}_{H\alpha_2} \\ &\quad \left. - \frac{e_* e_Z^2 - \kappa^2 (1 + \omega_*^2 + \omega_Z^2)}{4\omega_* \omega_Z \kappa^4} \hat{p}_{*\mu} \hat{p}_{Z\beta} \hat{r}_{H\alpha_1} \hat{r}_{H\alpha_2} \right]. \end{aligned} \quad (6.24)$$

The vertex terms contributing to the reduced helicity amplitudes, $\mathcal{T}_{\pm 1,0}$ and $\mathcal{T}_{0,\pm 1}$, lead to non-trivial $(1 + \cos^2 \theta) \sin^2 \vartheta$ and $\sin^2 \theta (1 + \cos^2 \vartheta)$ correlations, respectively, which are absent in the SM. Therefore, even though the invariant mass spectrum decreases linearly in κ , these non-trivial polar-angle correlations enable us to rule out effectively the spin-2 KK-graviton imposter assignment to the state. Explicitly, the normalized invariant-mass distribution is given by

$$\frac{d\mathcal{N}_H}{dm_\star} = \frac{m_\star [120m_\star^2 m_Z^2 - 10m_H^2 (m_H^2 - 3m_\star^2 - 2m_Z^2) \kappa^2 + m_H^2 (10m_H^2 + 2m_\star^2 + m_Z^2) \kappa^4]}{m_H^2 \mathcal{G}(\omega_Z) [(m_\star^2 - m_Z^2)^2 + m_Z^2 \Gamma_Z^2]} \kappa, \quad (6.25)$$

where the ω_Z -dependent function \mathcal{G} is given by

$$\begin{aligned} \mathcal{G}(\omega_Z) &= \omega_Z^2 (13 + 56\omega_Z^2 + 48\omega_Z^4) A_0(\omega_Z) + 4(3 + 8\omega_Z^2 + 20\omega_Z^4) A_1(\omega_Z) \\ &\quad - 2(9 - 10\omega_Z^2 + 12\omega_Z^4) A_2(\omega_Z) + 2(1 - 14\omega_Z^2) A_3(\omega_Z) \\ &\quad + (2 + 3\omega_Z^2) A_4(\omega_Z) + 2A_5(\omega_Z). \end{aligned} \quad (6.26)$$

Integrating the fully-correlated distribution over the invariant mass leads to the polar-angle correlation as

$$\begin{aligned} \frac{d^2 \mathcal{N}_H}{d \cos \theta d \cos \vartheta} &= \frac{9}{16} \left\{ \frac{\mathcal{G}_{LL}(\omega_Z)}{\mathcal{G}(\omega_Z)} \sin^2 \theta \sin^2 \vartheta + \frac{\mathcal{G}_{TT}(\omega_Z)}{\mathcal{G}(\omega_Z)} \frac{(1 + \cos^2 \theta)(1 + \cos^2 \vartheta)}{4} \right. \\ &\quad + \frac{\mathcal{G}_{TL}(\omega_Z)}{\mathcal{G}(\omega_Z)} \frac{(1 + \cos^2 \theta)}{2} \sin^2 \vartheta + \frac{\mathcal{G}_{LT}(\omega_Z)}{\mathcal{G}(\omega_Z)} \sin^2 \theta \frac{(1 + \cos^2 \vartheta)}{2} \\ &\quad \left. + \eta \ell \eta_f \frac{\mathcal{G}'_{TT}(\omega_Z)}{\mathcal{G}(\omega_Z)} \cos \theta \cos \vartheta \right\}, \end{aligned} \quad (6.27)$$

where the five ω_Z -dependent \mathcal{G} functions are given by

$$\begin{aligned} \mathcal{G}_{LL}(\omega_Z) &= \omega_Z^2 \left[(1 + 8\omega_Z^2 + 16\omega_Z^4) A_0(\omega_Z) + 8(1 + 4\omega_Z^2) A_1(\omega_Z) \right. \\ &\quad \left. + 2(7 - 4\omega_Z^2) A_2(\omega_Z) - 8A_3(\omega_Z) + A_4(\omega_Z) \right], \end{aligned} \quad (6.28)$$

$$\begin{aligned} \mathcal{G}_{TT}(\omega_Z) &= 2 \left[2\omega_Z^2 (3 + 8\omega_Z^4) A_0(\omega_Z) + 6(1 - 2\omega_Z^2 + 4\omega_Z^4) A_1(\omega_Z) \right. \\ &\quad \left. - (12 - 15\omega_Z^2 + 8\omega_Z^4) A_2(\omega_Z) + (7 - 10\omega_Z^2) A_3(\omega_Z) \right. \\ &\quad \left. - (2 - \omega_Z^2) A_4(\omega_Z) + A_5(\omega_Z) \right], \end{aligned} \quad (6.29)$$

$$\mathcal{G}_{TL}(\omega_Z) = 24\omega_Z^2 \left[\omega_Z^2 A_0(\omega_Z) + A_1(\omega_Z) \right], \quad (6.30)$$

$$\begin{aligned} \mathcal{G}_{LT}(\omega_Z) &= 6 \left[4\omega_Z^4 A_0(\omega_Z) + 4\omega_Z^2 A_1(\omega_Z) + (1 - 4\omega_Z^2) A_2(\omega_Z) \right. \\ &\quad \left. - 2A_3(\omega_Z) + A_4(\omega_Z) \right], \end{aligned} \quad (6.31)$$

$$\begin{aligned} \mathcal{G}'_{TT}(\omega_Z) &= -2 \left[2\omega_Z^2 (3 - 8\omega_Z^4) A_0(\omega_Z) + 6(1 - 2\omega_Z^2 - 4\omega_Z^4) A_1(\omega_Z) \right. \\ &\quad \left. - (12 + 3\omega_Z^2 - 8\omega_Z^4) A_2(\omega_Z) + 5(1 + 2\omega_Z^2) A_3(\omega_Z) \right. \\ &\quad \left. + (2 - \omega_Z^2) A_4(\omega_Z) - A_5(\omega_Z) \right], \end{aligned} \quad (6.32)$$

satisfying $\mathcal{G} = \mathcal{G}_{LL} + \mathcal{G}_{LT} + \mathcal{G}_{TL} + \mathcal{G}_{TT}$. Numerically, $\mathcal{G}_{LL} = 0.18 \mathcal{G}$, $\mathcal{G}_{LT} = 0.25 \mathcal{G}$, $\mathcal{G}_{TL} = 0.17 \mathcal{G}$, $\mathcal{G}_{TT} = 0.4 \mathcal{G}$, and $\mathcal{G}'_{TT} = -0.3 \mathcal{G}$. Integrating the polar-angle correlation over the polar angle ϑ leads to the normalized single polar-angle distribution as

$$\frac{d\mathcal{N}_H}{d \cos \theta} = \frac{3}{4} \left[\frac{\mathcal{G}_L(\omega_Z)}{\mathcal{G}(\omega_Z)} \sin^2 \theta + \frac{\mathcal{G}_T(\omega_Z)}{\mathcal{G}(\omega_Z)} \frac{(1 + \cos^2 \theta)}{2} \right], \quad (6.33)$$

where the two ω_Z -dependent functions $\mathcal{G}_{T,L}$ are given by

$$\begin{aligned} \mathcal{G}_L(\omega_Z) &= \omega_Z^2(1 + 32\omega_Z^2 + 16\omega_Z^4)A_0(\omega_Z) + 32\omega_Z^2(1 + \omega_Z^2)A_1(\omega_Z) \\ &\quad + 2(3 - 5\omega_Z^2 - 4\omega_Z^4)A_2(\omega_Z) - 4(3 + 2\omega_Z^2)A_3(\omega_Z) \\ &\quad + (6 + \omega_Z^2)A_4(\omega_Z), \end{aligned} \quad (6.34)$$

$$\begin{aligned} \mathcal{G}_T(\omega_Z) &= 2 \left[2\omega_Z^2(3 + 6\omega_Z^2 + 8\omega_Z^4)A_0(\omega_Z) + 6(1 + 4\omega_Z^4)A_1(\omega_Z) \right. \\ &\quad \left. - (12 - 15\omega_Z^2 + 8\omega_Z^4)A_2(\omega_Z) + (7 - 10\omega_Z^2)A_3(\omega_Z) \right. \\ &\quad \left. - (2 - \omega_Z^2)A_4(\omega_Z) + A_5(\omega_Z) \right], \end{aligned} \quad (6.35)$$

of which the sum is $\mathcal{G} = \mathcal{G}_T + \mathcal{G}_L$. Numerically, $\mathcal{G}_L = 0.43 \mathcal{G}$ and $\mathcal{G}_T = 0.57 \mathcal{G}$ for $\omega_Z = m_Z/m_H = 91/125 = 0.73$. The normalized azimuthal-angle distribution is given by

$$\frac{d\mathcal{N}_H}{d\varphi} = \frac{1}{2\pi} \left[1 + \frac{9\pi^2}{64} \eta_\ell \eta_f \frac{\mathcal{G}_1(\omega_Z)}{\mathcal{G}(\omega_Z)} \cos \varphi + \frac{\mathcal{G}_2(\omega_Z)}{\mathcal{G}(\omega_Z)} \cos 2\varphi \right], \quad (6.36)$$

where the expressions of two ω_Z -dependent functions $\mathcal{K}_{1,2}$ are

$$\begin{aligned} \mathcal{G}_1(\omega_Z) &= \omega_Z [16\omega_Z^2(1 + \omega_Z^2)B_0(\omega_Z) + (7 + 20\omega_Z^2)B_1(\omega_Z) \\ &\quad - (3 + 8\omega_Z^2)B_2(\omega_Z) - 5B_3(\omega_Z) + B_4(\omega_Z)], \end{aligned} \quad (6.37)$$

$$\begin{aligned} \mathcal{G}_2(\omega_Z) &= \frac{\sqrt{6}}{2} [4\omega_Z^4 A_0(\omega_Z) + \omega_Z^2(5 - 4\omega_Z^2)A_1(\omega_Z) \\ &\quad + (1 - 6\omega_Z^2)A_2(\omega_Z) - (2 - \omega_Z^2)A_3(\omega_Z) + A_4(\omega_Z)]. \end{aligned} \quad (6.38)$$

Numerically, $\mathcal{G}_1 = 0.17 \mathcal{G}$ and $\mathcal{G}_2 = 0.03 \mathcal{G}$ for $\omega_Z = m_Z/m_H = 91/125 = 0.73$. The integral-form definition and integrated expression of each $A_n(\omega_Z)$ with $n = 0$ to 5 are listed in Appendix B.

- **Spin ≥ 3 .** The number of the general HZ operators $[\mathcal{H}_{[\lambda_H, \lambda_Z]}^{1[HZ]}]$ with $j_0 = 1$ does not increase anymore. They are simply given by multiplying the general spin-2 HZ^*Z vertex $\Gamma_{\alpha_1 \alpha_2 \mu \beta}^{(2)}$ by a $(s_H - 2)$ -th order product of the re-scaled momentum $\hat{r}_H = \kappa \hat{r}$ as

$$\Gamma_{\alpha_1 \dots \alpha_{s_H} \mu \beta}^{(s_H)} = \kappa^{s_H - 2} [\Gamma_{\alpha_1 \alpha_2 \mu \beta}^{(2)}] \hat{r}_{\alpha_3} \dots \hat{r}_{\alpha_{s_H}}, \quad (6.39)$$

originating from the product $q_{\alpha_3} \dots q_{\alpha_{s_H}}$ with $q = k - k_Z = k_1 + k_2 - k_Z$. When contacted with the spin- s_H wave tensor, the extra $s_H - 2$ momenta give rise to a leading power $\kappa^{s_H - 2}$ in the helicity amplitudes. The invariant mass spectrum therefore decreases near the threshold in proportion to $\kappa^{2s_H - 3}$, i.e., with a power ≥ 3 for $s_H \geq 3$, in contrast to the single κ power behavior of the SM Higgs boson.

Reflecting all the detailed descriptions of the spin-0, spin-1, and spin-2 examples for the cascade decay $H \rightarrow Z^* Z \rightarrow \ell^- \ell^+ Z$ followed by the on-shell Z -boson decay $Z \rightarrow f \bar{f}$ with $\ell, f = e, \mu$, we show in Fig. 7 three characteristic distributions of the SM Higgs boson (black solid line), a pseudoscalar imposter (red dashed line), a spin-1 axial vector imposter (blue dot-dashed line) and a spin-2 KK graviton imposter (green dotted line), respectively. The left frame is for the normalized invariant-mass distribution while the middle and right frames are for the normalized single polar-angle distribution and the normalized azimuthal-angle distributions, respectively. In this numerical illustration, the Z -boson and H -boson masses are set to $m_Z = 91$ GeV and $m_H = 125$ GeV. The histograms for the SM Higgs boson shows the results from about 1800 events expected with essentially no kinematical cuts for an integrated luminosity of 300 fb^{-1} at the LHC. For a real experimental measurement of the 4-lepton signal events we refer to Ref. [101]. The pseudoscalar imposter can be clearly vetoed by each of the three distributions, the spin-1 axial-vector imposter can be vetoed by the normalized azimuthal-angle distribution. In contrast, the mimicry of the SM Higgs boson by the spin-2 KK graviton imposter in all three distributions poses a challenge in definitively distinguishing between the two. To achieve a clear distinction, more sophisticated discriminatory distributions are required.

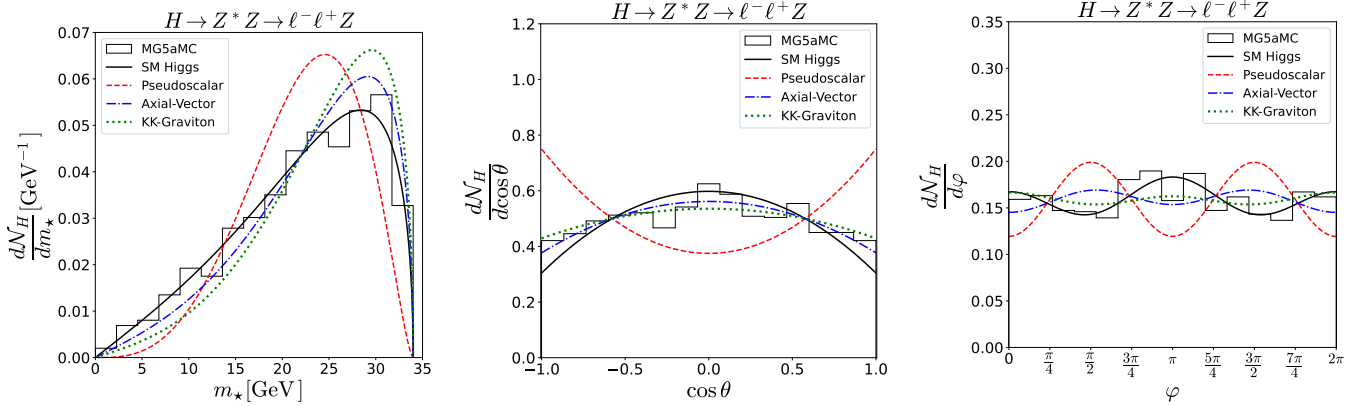


Figure 7: *Three characteristic distributions of the SM Higgs boson (black solid line), a pseudoscalar imposter (red dashed line), a spin-1 axial vector imposter (blue dot-dashed line), and a spin-2 KK graviton imposter (green dotted line), respectively. The left frame is the normalized invariant-mass distribution while the middle and right frames are the single polar-angle and azimuthal-angle distributions, respectively. The Z -boson and H -boson masses are set to $m_Z = 91$ GeV and $m_H = 125$ GeV. The histograms for the SM Higgs boson show the results from about 1800 four-lepton events expected with essentially, no kinematical cuts for an integrated luminosity of 300 fb^{-1} at the LHC.*

One of the powerful quantities for vetoing the spin-2 KK graviton imposter against the SM Higgs boson is the polar-angle correlation. As illustrated in Fig. 8, the double polar-angle correlation for the SM Higgs boson (left frame) is clearly distinct from that for the spin-2 KK graviton imposter, enabling us to veto the spin-2 imposter unambiguously. The slightly tilted distribution is due to the $\eta_e \eta_f \cos \theta \cos \vartheta$ originating from the parity-violating $Z^* \ell \ell$ and $Z f \bar{f}$ couplings.

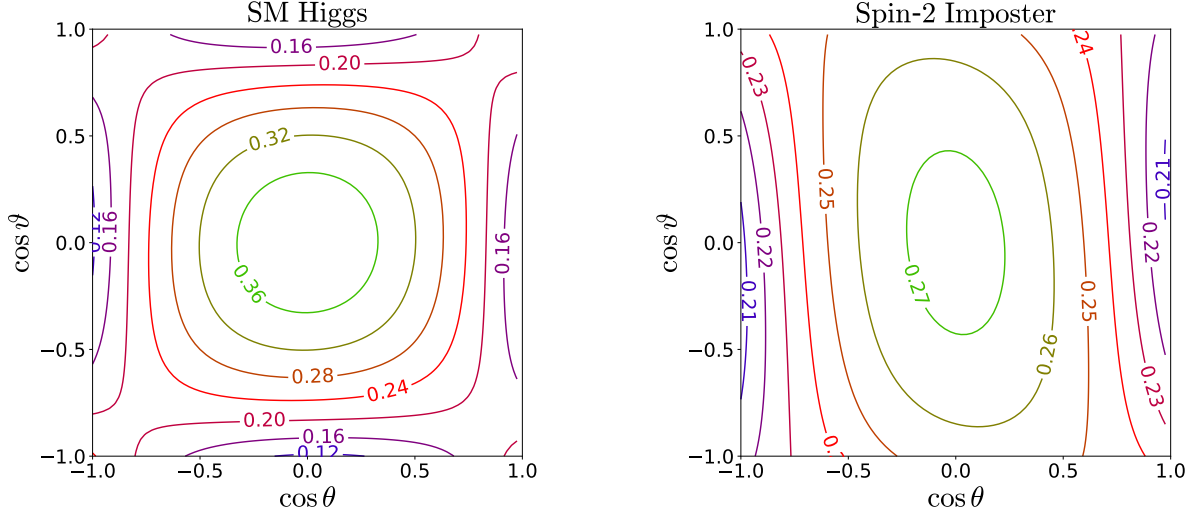


Figure 8: Fully-correlated polar-angle distribution for the SM Higgs boson (left) and the spin-2 KK-graviton imposter (right), respectively. As before, the Z -boson and H -boson masses are set to be $m_Z = 91$ GeV and $m_H = 125$ GeV, respectively.

6.2 The case with contact terms of maximal j_0

Generally, the four-point $H\ell\ell Z$ interactions contain not only $j_0 = 1$ terms but also $j_0 > 1$ terms for the H spin $s_H \geq 1$, arising from new physics beyond the SM. They can be generated by simple 4-point angle-independent contact terms or terms describing the interactions of ℓ^\mp directly either with the H boson or the on-shell Z boson. As described before, apart from the purely angle-dependent Wigner d functions, the reduced helicity amplitudes $\mathcal{T}_{\lambda_H; \sigma, \lambda_Z}^{[H\ell\ell Z]}(m_*, \kappa \cos \theta)$ in Eq. (4.14) is in general dependent on the combination $\kappa \cos \theta$ vanishing at the threshold with $m_* = m_H - m_Z$. In contrast, each contact term with maximal j_0 generates a constant reduced helicity amplitude.

- **Spin 0.** If the H particle is spinless, the j_0 value is fixed to be 1. Therefore, the parity-even case with contact terms could imitate the case with the SM Higgs boson for the polar and azimuthal angular distributions. However, with no virtual Z^* exchange, the overall pattern of the two-lepton invariant mass distribution is qualitatively different from the SM case for which the distribution varies in proportion to $\omega_Z^4/(\omega_Z^2 - \omega_*^2)^2$ as ω_* approaches the value of $1 - \omega_Z = 0.27$ at the threshold. For example, the contact term of the parity-even $U_{\mu\beta}^+ + U_{\mu\beta}^-$ form leads to the normalized invariant-mass distribution as

$$\frac{d\mathcal{N}_H}{dm_*} = \frac{m_*^3}{m_H^4 \mathcal{C}_1(\omega_Z)} \kappa \quad \text{with} \quad \mathcal{C}_1(\omega_Z) = \omega_Z^2 A_2(\omega_Z) + A_3(\omega_Z), \quad (6.40)$$

when the theory is nearly P invariant. The explicit form of $\mathcal{C}_1(\omega_Z)$ is given in Appendix B. The single polar-angle distribution due to the contact term is of the simple form

$$\frac{d\mathcal{N}_H}{d\cos \theta} = \frac{3}{8}(1 + \cos^2 \theta), \quad (6.41)$$

clearly different from that of the SM Higgs boson. On the other hand, the parity-odd pseudoscalar case can be ruled out unambiguously by confirming not only the invariant mass but also and the polar and azimuthal angle correlations characterizing the SM Higgs boson, as before.

- **Spin 1.** If the H spin is 1, the general spin-1 four-point vertex tensor contains two non-trivial $j_0 = 2$ contact vertex terms as

$$\omega_\star W_\sigma^{\mu_1} \hat{l}^{\mu_2} U_{\alpha\mu_1}^\pm U_{\beta\mu_2}^\pm, \quad (6.42)$$

which correspond to the H and Z helicity combinations, $(\pm 2, \mp 1)$, generating the distributions of the maximal j_0 value of 2. Because each of them contains two terms with no momentum dependence, the corresponding normalized invariant-mass distribution decreases steeply as

$$\frac{d\mathcal{N}_H}{dm_\star} = \frac{m_\star^5}{m_H^4 \mathcal{C}_2(\omega_Z)} \kappa, \quad \text{with} \quad \mathcal{C}_2(\omega_Z) = \omega_Z^4 A_2(\omega_Z) + 2\omega_Z^2 A_3(\omega_Z) + A_4(\omega_Z), \quad (6.43)$$

which is linearly proportional to κ near the threshold. For the explicit form of $\mathcal{C}_2(\omega_Z)$ we refer to Appendix B. Nevertheless, due to the absence of any intermediate state, the global feature of the invariant mass distribution will be qualitatively different from the SM case.

Furthermore, combined with the $\ell^-\ell^+$ system, the contact terms in Eq. (6.42) generate the non-trivial Wigner d functions

$$d_{\pm 2, \sigma}^2(\theta) = -\frac{1}{2} \sin \theta (1 \pm \sigma \cos \theta) \quad \text{with} \quad \sigma = \pm 1, \quad (6.44)$$

as shown in Eq. (4.18). Therefore, the single polar-angle distribution due to the $j_0 = 2$ contact terms in the spin-1 case is given by

$$\frac{d\mathcal{N}_H}{d \cos \theta} = \frac{5}{8} \sin^2 \theta (1 + \cos^2 \theta), \quad (6.45)$$

which is distinctly different from that of the SM Higgs boson.

- **Spin 2.** If the H spin is 2, we have eight ($8 = 2 \times 4$) $j_0 = 2$ terms and there are four ($4 = 2 \times 2$) $j_0 = 3$ terms as shown in Tab. 2. Every $j_0 = 2$ term involves at least one power of momentum so that every helicity amplitude vanishes near threshold linearly in κ , distinct from the SM. On the other hand, each of the HZ operators with $j_0 = 3$ contains a momentum-free term leading to non-zero helicity amplitudes at the threshold. The contact terms consisting of the HZ operators with $j_0 = 3$ generate the following normalized invariant-mass distribution:

$$\frac{d\mathcal{N}_H}{dm_\star} = \frac{m_\star^7}{m_H^8 \mathcal{C}_3(\omega_Z)} \kappa, \quad (6.46)$$

where the ω_Z -dependent integral function is given by

$$\mathcal{C}_3(\omega_Z) = \omega_Z^6 A_2(\omega_Z) + 3\omega_Z^4 A_3(\omega_Z) + 3\omega_Z^2 A_4(\omega_Z) + A_5(\omega_Z), \quad (6.47)$$

of which the explicit form is given in Appendix B. The normalized invariant-mass distribution decreases steeply near the threshold.

Combined with the $\ell^-\ell^+$ system, the terms generate the helicity amplitudes proportional to the non-trivial Wigner d functions

$$d_{\pm 3, \sigma}^3(\theta) = \frac{\sqrt{15}}{8} \sin^2 \theta (1 \pm \sigma \cos \theta) \quad \text{with } \sigma = \pm 1. \quad (6.48)$$

Therefore, the normalized single polar-angle distribution due to the $j_0 = s_H + 1 = 3$ contact term in the spin-2 case is given by

$$\frac{d\mathcal{N}_H}{d \cos \theta} = \frac{105}{128} \sin^4 \theta (1 + \cos^2 \theta), \quad (6.49)$$

which is distinctly different from that of the SM Higgs boson.

Figure 9 shows the invariant-mass distribution on the left frame and the single polar-angle distribution on the right frame of the cases only with the $s_H = 0$ contact (red dashed line), $s_H = 1$ contact (blue dot-dashed line), and $s_H = 2$ contact (green dotted line) terms, each of which corresponds to the maximally-allowed j_0 value of 1, 2, or 3, respectively, in comparison with the SM Higgs boson (black solid line). Even in the spin-0 case, the invariant-mass distribution is different from that of the SM Higgs boson, with more prominent difference for the higher-spin case, as shown in the left frame of Fig. 9. The single polar-angle distribution due to any maximal- j_0 contact term is also very different from that of the SM Higgs boson as clearly shown in the right frame of Fig. 9.

- **Spin ≥ 3 .** Except for four special cases to be mentioned shortly, every term involves at least one power of momentum so that the invariant mass distribution vanishes near the threshold linearly at least in κ^3 , distinct from the SM case. The four HZ operators with no momentum dependence are

$$[\mathcal{H}_{\pm s_H, \pm 1}^{(s_H+1)[HZ]}] = [U_H^\pm]^{s_H} [U_Z^\pm], \quad (6.50)$$

$$[\mathcal{H}_{\pm s_H, \mp 1}^{(s_H-1)[HZ]}] = [U_H^\pm]^{s_H-1} [U_{HZ}^\pm]. \quad (6.51)$$

Combining these HZ and $\ell\ell$ operators with all the wave functions generates the helicity amplitudes with the following non-trivial Wigner d functions (apart from some $\kappa \cos \theta$ -dependent form factors)

$$d_{\pm(s_H+1), \sigma}^{(s_H+1)}(\theta) \propto (\sin \theta)^{s_H} (1 \pm \sigma \cos \theta), \quad (6.52)$$

$$d_{\pm(s_H-1), \sigma}^{(s_H-1)}(\theta) \propto (\sin \theta)^{s_H-2} (1 \pm \sigma \cos \theta). \quad (6.53)$$

Clearly, for $s_H \geq 3$, the non-trivial power terms of $\sin \theta$ render the single polar-angle distribution significantly different from that of the SM Higgs boson with the spin value of $s_H = 0$. Explicitly, the normalized invariant-mass distribution for the maximal $j_0 = s_H + 1$ term is given by

$$\frac{d\mathcal{N}_H}{dm_\star} = \frac{m_\star^{2s_H+3}}{m_H^{2(s_H+2)} \mathcal{C}_n(\omega_Z)} \kappa, \quad (6.54)$$

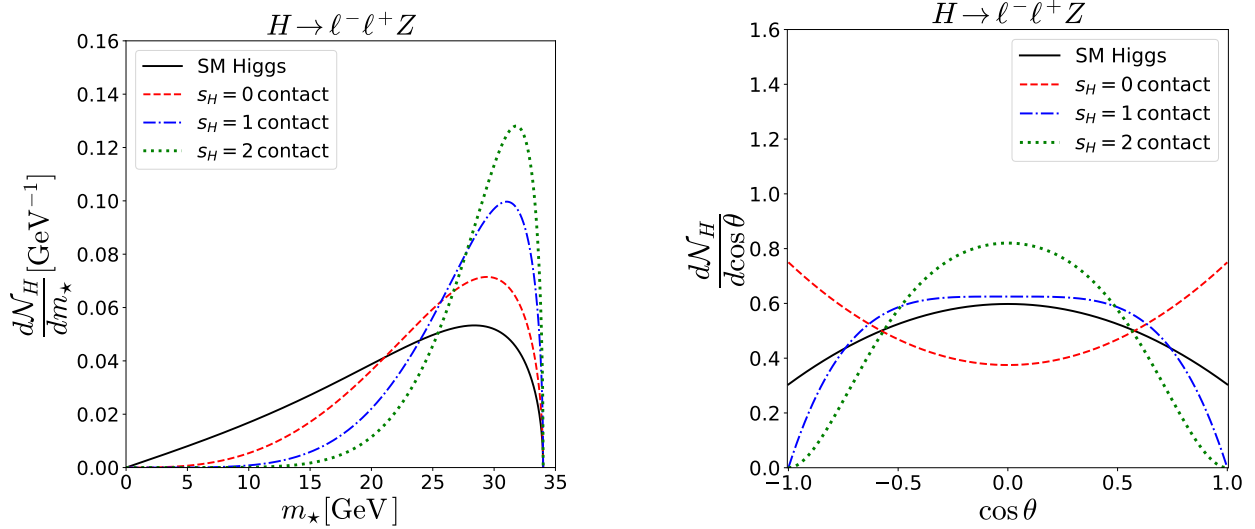


Figure 9: Invariant-mass (left frame) and single polar-angle (right frame) distributions of the cases only with the $s_H = 0$ contact (red dashed line), $s_H = 1$ contact (blue dot-dashed line), and $s_H = 2$ contact (green dotted line) terms corresponding to the maximal j_0 values of 1, 2, and 3, respectively, in comparison with the SM Higgs boson (black solid line). Both distributions due to the maximal- j_0 contact terms in any integer-spin case are clearly distinct from those of the SM Higgs boson.

where the ω_Z -dependent integral function $\mathcal{C}_n(\omega_Z)$ is defined in general by

$$\mathcal{C}_n(\omega_Z) = \int_0^{1-\omega_Z} d\omega_* \omega_*^{2n+1} \kappa, \quad (6.55)$$

in terms of the non-negative integer n , which can be expressed as a linear combination of the A integral functions defined in Eq. (B.1).

The maximal- j_0 term with $j_0 = s_H + 1$ leads to the corresponding normalized single polar-angle distribution as

$$\frac{d\mathcal{N}_H}{d\cos\theta} = \frac{(2s_H + 3)}{2^{2s_H+2}(s_H + 2)} \frac{(2s_H + 1)!}{(s_H!)^2} (\sin\theta)^{2s_H} (1 + \cos^2\theta), \quad (6.56)$$

valid for any non-negative integer spin s_H including $s_H = 0, 1$ and 2 and manifestly different from the SM Higgs case for positive values of s_H .

7 Summary and conclusion

We have devised an effective and systematic algorithm for constructing covariant four-point $H\ell\ell Z$ vertices pertaining to a massive particle H with an arbitrary integer spin value. This algorithm leverages a direct correspondence between helicity formalism and covariant representation to delineate the 3-body decay channel $H \rightarrow \ell^- \ell^+ Z$. By upholding chirality conservation and disregarding the

negligible masses of light leptons (where $m_\ell = 0$ for $\ell = e, \mu$), our algorithm stands as a natural yet intriguing extension of the previously established methodology for systematically constructing all-encompassing three-point vertices detailed across a series of publications [71–73].

The methodically developed general covariant four-point $H\ell\ell Z$ vertices serve as a robust tool for systematically discerning the spin and parity attributes of the SM Higgs boson, particularly within the realm of one of its key decay channels, the three-body decay $H \rightarrow \ell^-\ell^+Z$, where $\ell = e, \mu$, observable at the LHC. This analytical approach, centered around the general covariant four-point vertex, surpasses preceding studies on Higgs spin and parity determination. Furthermore it accommodates a much broader spectrum of analyses, encompassing all the effectively allowed 4-point $H\ell\ell Z$ interactions.

We have confirmed firmly that threshold effects and angular correlations can be adopted to determine spin and parity unambiguously in the significantly expanded setting, though high event rates are required for the analysis in practice. These essential conclusions can be covered by summarizing the analyses in a few characteristic points. The SM Higgs boson possesses a unique invariant-mass spectrum with its steeply-decreasing threshold behavior and also its unique polar-angle and azimuthal-angle correlations, characterizing its spin-zero and parity-even nature and its messenger role of EWSB. With the observation of the unique global spectrum and the steep decrease near the kinematical limit for the SM Higgs boson, we can rule out all the other spin and/or parity assignments to the H boson not only in the standard two-step cascade decay but also in all the decay processes involving the general four-point interactions by checking out the two-lepton invariant-mass distribution and the single and/or correlated polar-angle and azimuthal-angle distributions.

The selection rules proposed so far for confirming the spinless nature and even parity of the SM Higgs boson unambiguously through its 3-body decay $H \rightarrow \ell^-\ell^+Z$ can be supplemented by observations specific to two cases. By observing non-zero $H\gamma\gamma$ and Hgg couplings, the unit-spin assignment of $s_H = 1$ can elegantly ruled out in particular and every odd-spin assignment in general by Landau-Yang theorem [49, 52, 102–104].

The formalism developed in the present work can be extended to exclude mixed normality states effortlessly. The differential decay width in the CP -noninvariant theory proves to be more intricate, compared to that in the CP -invariant theory. Particularly, the double polar-angle distribution is adjusted to incorporate linear terms that are proportional to either $\cos\theta$ or $\cos\vartheta$, demonstrating CP violation [93–97]. Despite the inherent complexity, the analysis for determining the spin of the SM Higgs particle by ruling out all potential imposter scenarios follows the same procedure as in the case of fixed normality, since the general 4-point vertex is simply the sum of even and odd normality tensors.

The general algorithm for constructing the covariant four-point $H\ell\ell Z$ vertex with H of any integer spin enables us to work out a similar unambiguous and powerful procedure for identifying the spin and parity of the SM Higgs boson in the so-called Higgs-strahlung process $e^-e^+ \rightarrow ZH$, topologically equivalent to the 3-body decay $H \rightarrow e^-e^+Z$. This investigation is currently under rigorous examination and is anticipated to reach completion soon.

Absolutely, even after confirming the spinless nature of the H boson, the general Lorentz-covariant four-point vertex structure serves as a robust foundation not only for delving deeper into the 3-body decay process of the spin-0 Higgs boson but also for exploring a range of theoretical considerations such as unitarity and potential (hidden) discrete and/or gauge symmetries through diverse two-to-

two scattering and three-body decay processes [105–109].

Before closing, we mention that it will be extremely valuable to develop a computation package implementing our general analytic algorithm fully so as to identify the spin and parity of the SM Higgs boson and to investigate various new physics phenomena involving any integer-spin massive particle automatically with real experimental data delivered at not only the LHC but also the high-luminosity LHC (HL-LHC) [26, 27, 110].

Acknowledgments

This work is supported by the Basic Research Laboratory Program of the National Research Foundation of Korea (Grant No. NRF-2022R1A4A5030362 for SYC and DWK). SYC is supported in part by the Basic Science Research Program of Ministry of Education through the National Research Foundation of Korea (Grant No. NRF-2022R1I1A3071226). JJ is supported by a KIAS Individual Grant (QP090001) via the Quantum Universe Center at Korea Institute for Advanced Study.

A Various formulas for evaluating helicity amplitudes

It is necessary to derive the helicity amplitudes (4.14) for the three-body decay process $H \rightarrow \ell^- \ell^+ Z$ by calculating the corresponding amplitudes (4.1) expressed in terms of the general HZ and $\ell\ell$ operators before investigating all the invariant-mass and angular correlations systematically. We collect in this appendix A a set of analytic formulas which can be exploited for calculating the helicity amplitudes systematically and efficiently.

Firstly, for the sake of self-containment and concreteness, we re-write down all the relevant normalized momenta introduced in the main text collectively:

$$\hat{p} = (1, 0, 0, 0) \quad \Rightarrow \quad \hat{p}_{\star\mu} = 2\omega_{\star}\hat{p}_{\mu}, \quad \hat{p}_{Z\beta} = 2\omega_Z\hat{p}_{\beta}, \quad (\text{A.1})$$

$$\hat{r} = (0, 0, 0, 1) \quad \Rightarrow \quad \hat{r}_{H\alpha} = \kappa\hat{r}_{\alpha}, \quad (\text{A.2})$$

$$\hat{k} = \frac{1}{2\omega_{\star}}(e_{\star}, 0, 0, \kappa) \quad \text{and} \quad \hat{l} = \frac{1}{2\omega_{\star}}(\kappa \cos \theta, 2\omega_{\star} \sin \theta, 0, e_{\star} \cos \theta), \quad (\text{A.3})$$

along with the normalized chirality-conserving $\ell^- \ell^+$ lepton current \hat{l}_{\pm}

$$\hat{l}_{\pm} = \pm \frac{1}{2\sqrt{2}\omega_{\star}}(\kappa \sin \theta, -2\omega_{\star} \cos \theta, \pm 2i\omega_{\star}, e_{\star} \sin \theta), \quad (\text{A.4})$$

in the H rest frame. Here, we introduce the normalized masses, $\omega_{\star} = m_{\star}/m_H$ and $\omega_Z = m_Z/m_H$, defining the kinematic variables, $e_Z = 1 + \omega_Z^2 - \omega_{\star}^2$ and $e_{\star} = 1 - \omega_Z^2 + \omega_{\star}^2$, and the polar angle θ of the flight direction of the lepton ℓ^- in the $\ell^- \ell^+$ rest frame with respect to the original 3-momentum of the $\ell^- \ell^+$ system in the kinematic configuration in Fig. 2 where the H boson is at rest. Contracting the newly-defined momenta and their corresponding longitudinal polarization vectors or normalized

momenta lead to the following set of non-trivial relations

$$\hat{r}_H \cdot \epsilon(p_H, \lambda_H) = -\kappa \delta_{\lambda_H, 0} \quad \text{and} \quad \epsilon^*(k_Z, \lambda_Z) \cdot \hat{p}_Z = \kappa \delta_{\lambda_Z, 0}, \quad (\text{A.5})$$

$$\hat{p}_\star \cdot \hat{l}_\pm = \pm \frac{1}{\sqrt{2}} \kappa \sin \theta \quad \text{and} \quad \hat{p}_\star \cdot \hat{l} = \kappa \cos \theta, \quad (\text{A.6})$$

where the longitudinal H and Z polarization vectors are explicitly given by

$$\epsilon(p_H, 0) = (0, 0, 0, 1) \quad \text{and} \quad \epsilon(k_Z, 0) = \frac{1}{2\omega_Z} (\kappa, 0, 0, -e_Z). \quad (\text{A.7})$$

It is worthwhile to note that each contracted term is linearly proportional to the kinematical factor κ , becoming zero at the kinematical threshold of $\omega_\star = 1 - \omega_Z$.

Secondly, in the same kinematic configuration of Fig. 2, the basic operator U^\pm in any pair of three 4-vector indices $\{\alpha, \mu, \beta\}$, is given in a 4×4 matrix form by

$$U^\pm = -\frac{1}{2} \begin{pmatrix} 0 & 0 & 0 & 0 \\ 0 & 1 & \mp i & 0 \\ 0 & \pm i & 1 & 0 \\ 0 & 0 & 0 & 0 \end{pmatrix} = -|p_H, \pm 1\rangle \langle p_H, \pm 1| = -|k_Z, \mp 1\rangle \langle k_Z, \mp 1|, \quad (\text{A.8})$$

which is corresponding to the tensor product of the transverse polarization 4-vector, $\epsilon(p_H, \pm 1)$ or $\epsilon(k_Z, \mp 1)$, of which the expression is given by

$$\epsilon(p_H, \pm 1) = \epsilon^*(k_Z, \pm 1) = \frac{1}{\sqrt{2}} (0, \mp 1, -i, 0), \quad (\text{A.9})$$

respectively, and its Hermitian conjugate vector, $\epsilon^*(p_H, \pm 1)$ or $\epsilon^*(k_Z, \mp 1)$. Contracting the tensor operator with any pair of the transverse H and Z polarization vectors, the normalized lepton current \hat{l}_σ and the normalized momentum \hat{l} leads to the following set of non-trivial relations:

$$\epsilon^*(k_Z, \lambda_Z) \cdot U^\pm \cdot \epsilon(p_H, \lambda_H) = -\delta_{\lambda_H, \pm 1} \delta_{\lambda_Z, \mp 1}, \quad (\text{A.10})$$

$$\hat{l}_\sigma \cdot U^\pm \cdot \epsilon(p_H, \lambda_H) = \mp \frac{1}{2} (1 \pm \sigma \cos \theta) \delta_{\lambda_H, \pm 1}, \quad (\text{A.11})$$

$$\hat{l} \cdot U^\pm \cdot \epsilon(p_H, \lambda_H) = \frac{1}{\sqrt{2}} \sin \theta \delta_{\lambda_H, \pm 1}, \quad (\text{A.12})$$

$$\hat{l}_\sigma \cdot U^\pm \cdot \epsilon^*(k_Z, \lambda_Z) = \mp \frac{1}{2} (1 \pm \sigma \cos \theta) \delta_{\lambda_Z, \mp 1}, \quad (\text{A.13})$$

$$\hat{l} \cdot U^\pm \cdot \epsilon^*(k_Z, \lambda_Z) = \frac{1}{\sqrt{2}} \sin \theta \delta_{\lambda_Z, \mp 1}, \quad (\text{A.14})$$

of which all terms depend only on the polar angle θ .

B Integral functions

In order to facilitate the integration of various ω_* -dependent functions and to express the results in a compact form, we introduce two types of ω_Z -dependent integral functions, A_n and B_n , as

$$A_n(\omega_Z) = \int_0^{1-\omega_Z} d\omega_* \frac{\omega_* \kappa}{(\omega_*^2 - \omega_Z^2)^{2-n}}, \quad (\text{B.1})$$

$$B_n(\omega_Z) = \int_0^{1-\omega_Z} d\omega_* \frac{\omega_*^2 \kappa}{(\omega_*^2 - \omega_Z^2)^{2-n}}, \quad (\text{B.2})$$

for a non-negative integer n .

Firstly, the expressions of six integral functions A_n from $n = 0$ to $n = 5$ are given explicitly by

$$A_0(\omega_Z) = -\frac{1 - \omega_Z^2}{2\omega_Z^2} + \frac{1}{2\sqrt{4\omega_Z^2 - 1}} \cos^{-1} \left(\frac{3\omega_Z^2 - 1}{2\omega_Z^3} \right) - \frac{1}{2} \ln \omega_Z, \quad (\text{B.3})$$

$$A_1(\omega_Z) = -\frac{1 - \omega_Z^2}{2} + \frac{\sqrt{4\omega_Z^2 - 1}}{2} \cos^{-1} \left(\frac{3\omega_Z^2 - 1}{2\omega_Z^3} \right) + \frac{1}{2} \ln \omega_Z, \quad (\text{B.4})$$

$$A_2(\omega_Z) = \frac{1 - \omega_Z^2}{4} (1 + \omega_Z^2) + \omega_Z^2 \ln \omega_Z, \quad (\text{B.5})$$

$$A_3(\omega_Z) = -\frac{1 - \omega_Z^2}{12} (2\omega_Z^4 - 7\omega_Z^2 - 1) + \omega_Z^2 \ln \omega_Z, \quad (\text{B.6})$$

$$A_4(\omega_Z) = \frac{1 - \omega_Z^2}{24} (3\omega_Z^6 - 5\omega_Z^4 + 25\omega_Z^2 + 1) + \omega_Z^2 (1 + \omega_Z^2) \ln \omega_Z, \quad (\text{B.7})$$

$$A_5(\omega_Z) = -\frac{1 - \omega_Z^2}{120} (12\omega_Z^8 - 13\omega_Z^6 - 73\omega_Z^4 - 163\omega_Z^2 - 3) + \omega_Z^2 (1 + 3\omega_Z^2) \ln \omega_Z, \quad (\text{B.8})$$

with $\omega_Z = m_Z/m_H = 0.73$ less than unity.

Secondly, the expressions of five integral functions B_n from $n = 0$ to $n = 4$ are given explicitly in terms of three types of elliptic integrals by

$$B_0(\omega_Z) = \frac{2\omega_Z^2 + 6\omega_Z - 1}{2(1 + \omega_Z)} K(r_Z) - \frac{3(1 + \omega_Z)}{2} E(r_Z) + \frac{6\omega_Z^2 - 1}{2\omega_Z^2(1 + \omega_Z)} \Pi(n_Z, r_Z), \quad (\text{B.9})$$

$$B_1(\omega_Z) = \frac{\omega_Z(2\omega_Z^2 - 11\omega_Z - 4)}{3(1 + \omega_Z)} K(r_Z) + \frac{(1 + \omega_Z)(2 - \omega_Z^2)}{3} E(r_Z) + \frac{4\omega_Z^2 - 1}{1 + \omega_Z} \Pi(n_Z, r_Z), \quad (\text{B.10})$$

$$B_2(\omega_Z) = -\frac{2(1 + \omega_Z)}{15} \left[2\omega_Z(\omega_Z^2 + 6\omega_Z + 1)K(r_Z) - (\omega_Z^4 + 14\omega_Z^2 + 1)E(r_Z) \right], \quad (\text{B.11})$$

$$B_3(\omega_Z) = \frac{2(1 + \omega_Z)}{105} \left[2\omega_Z(4\omega_Z^4 - 6\omega_Z^3 - 19\omega_Z^2 - 48\omega_Z - 3)K(r_Z) - (4\omega_Z^6 - 27\omega_Z^4 - 118\omega_Z^2 - 3)E(r_Z) \right], \quad (\text{B.12})$$

$$B_4(\omega_Z) = -\frac{2(1 + \omega_Z)}{315} \left[2\omega_Z(8\omega_Z^6 - 12\omega_Z^5 - 12\omega_Z^4 + 180\omega_Z^3 + 105\omega_Z^2 + 150\omega_Z + 5)K(r_Z) - (8\omega_Z^8 - 28\omega_Z^6 + 453\omega_Z^4 + 410\omega_Z^2 + 5)E(r_Z) \right], \quad (\text{B.13})$$

with $n_Z = (1 - \omega_Z)/\omega_Z$, and $r_Z = (1 - \omega_Z)/(1 + \omega_Z)$. The first-, second- and third-kind complete elliptic integrals are defined by

$$K(r_Z) = \int_0^{\pi/2} \frac{d\theta}{\sqrt{1 - r_Z^2 \sin^2 \theta}}, \quad (\text{B.14})$$

$$E(r_Z) = \int_0^{\pi/2} \sqrt{1 - r_Z^2 \sin^2 \theta} d\theta, \quad (\text{B.15})$$

$$\Pi(n_Z, r_Z) = \int_0^{\pi/2} \frac{1}{1 - n_Z^2 \sin^2 \theta} \frac{d\theta}{\sqrt{1 - r_Z^2 \sin^2 \theta}}, \quad (\text{B.16})$$

in a definite integral form.

The invariant-mass and angular distributions for the pure contact interactions without any intermediate virtual Z exchange can be expressed in a compact manner by introducing another set of ω_Z -dependent integral functions as

$$\mathcal{C}_n(\omega_Z) = \int_0^{1-\omega_Z} d\omega_* \omega_*^{2n+1} \kappa. \quad (\text{B.17})$$

Explicitly, the expressions of the integrals, $\mathcal{C}_n(\omega_Z)$, for $n = 1, 2, 3$ are given by,

$$\mathcal{C}_1(\omega_Z) = \frac{1 - \omega_Z^4}{4} + \omega_Z^2 \ln \omega_Z, \quad (\text{B.18})$$

$$\mathcal{C}_2(\omega_Z) = \frac{1 - \omega_Z^2}{12} (1 + 10\omega_Z^2 + \omega_Z^4) + \omega_Z^2 (1 + \omega_Z^2) \ln \omega_Z, \quad (\text{B.19})$$

$$\mathcal{C}_3(\omega_Z) = \frac{1 - \omega_Z^2}{24} (1 + 29\omega_Z^2 + 29\omega_Z^4 + \omega_Z^6) + \omega_Z^2 (1 + 3\omega_Z^2 + \omega_Z^4) \ln \omega_Z. \quad (\text{B.20})$$

As shown explicitly with $\mathcal{C}_{1,2,3}$ in the main text, every \mathcal{C} integral function can be expressed as a linear combination of the A integral functions defined in Eq. (B.1).

References

- [1] S. L. Glashow. Partial Symmetries of Weak Interactions. *Nucl. Phys.*, 22:579–588, 1961.
- [2] Steven Weinberg. A Model of Leptons. *Phys. Rev. Lett.*, 19:1264–1266, 1967.
- [3] Abdus Salam. Weak and Electromagnetic Interactions. *Conf. Proc. C*, 680519:367–377, 1968.
- [4] H. Fritzsch, Murray Gell-Mann, and H. Leutwyler. Advantages of the Color Octet Gluon Picture. *Phys. Lett. B*, 47:365–368, 1973.
- [5] Georges Aad et al. Observation of a new particle in the search for the Standard Model Higgs boson with the ATLAS detector at the LHC. *Phys. Lett. B*, 716:1–29, 2012.
- [6] Serguei Chatrchyan et al. Observation of a New Boson at a Mass of 125 GeV with the CMS Experiment at the LHC. *Phys. Lett. B*, 716:30–61, 2012.

- [7] Steven Weinberg. Essay: Half a Century of the Standard Model. *Phys. Rev. Lett.*, 121(22):220001, 2018.
- [8] R. L. Workman et al. Review of Particle Physics. *PTEP*, 2022:083C01, 2022.
- [9] Steven Weinberg. Effective field theory, past and future. *Int. J. Mod. Phys. A*, 31(06):1630007, 2016.
- [10] Ilaria Brivio and Michael Trott. The Standard Model as an Effective Field Theory. *Phys. Rept.*, 793:1–98, 2019.
- [11] Aneesh V. Manohar. Introduction to Effective Field Theories. 4 2018.
- [12] Steven Weinberg. On the Development of Effective Field Theory. *Eur. Phys. J. H*, 46(1):6, 2021.
- [13] C. P. Burgess. *Introduction to Effective Field Theory*. Cambridge University Press, 12 2020.
- [14] Michèle Levi. A Theory of Theories. *CERN Cour.*, 63(1):37–40, 2023.
- [15] All things eft. Talks can be viewed at <https://www.youtube.com/@allthingseft806> which brings together each week the worldwide community of EFT practitioners.
- [16] F. Englert and R. Brout. Broken Symmetry and the Mass of Gauge Vector Mesons. *Phys. Rev. Lett.*, 13:321–323, 1964.
- [17] Peter W. Higgs. Broken Symmetries and the Masses of Gauge Bosons. *Phys. Rev. Lett.*, 13:508–509, 1964.
- [18] G. S. Guralnik, C. R. Hagen, and T. W. B. Kibble. Global Conservation Laws and Massless Particles. *Phys. Rev. Lett.*, 13:585–587, 1964.
- [19] John F. Gunion, Howard E. Haber, Gordon L. Kane, and Sally Dawson. *The Higgs Hunter’s Guide*, volume 80. 2000.
- [20] Abdelhak Djouadi. The Anatomy of electro-weak symmetry breaking. I: The Higgs boson in the standard model. *Phys. Rept.*, 457:1–216, 2008.
- [21] D. de Florian et al. Handbook of LHC Higgs Cross Sections: 4. Deciphering the Nature of the Higgs Sector. 2/2017, 10 2016.
- [22] Gavin P. Salam, Lian-Tao Wang, and Giulia Zanderighi. The Higgs boson turns ten. *Nature*, 607(7917):41–47, 2022.
- [23] Georges Aad et al. A detailed map of Higgs boson interactions by the ATLAS experiment ten years after the discovery. *Nature*, 607(7917):52–59, 2022. [Erratum: *Nature* 612, E24 (2022)].
- [24] Armen Tumasyan et al. A portrait of the Higgs boson by the CMS experiment ten years after the discovery. *Nature*, 607(7917):60–68, 2022. [Erratum: *Nature* 623, (2023)].

- [25] Giacomo Ortona. The Higgs boson couplings: past, present, and future. The relationships between Higgs boson and other known particles as measured by current and future experiments. *Front. in Phys.*, 11:1230737, 2023.
- [26] Michelangelo Mangano. TASI Lectures on Future Colliders. *PoS*, TASI2018:008, 2019.
- [27] Vladimir Shiltsev and Frank Zimmermann. Modern and Future Colliders. *Rev. Mod. Phys.*, 93:015006, 2021.
- [28] S. Y. Choi, D. J. Miller, M. M. Muhlleitner, and P. M. Zerwas. Identifying the Higgs spin and parity in decays to Z pairs. *Phys. Lett. B*, 553:61–71, 2003.
- [29] A. Bredenstein, Ansgar Denner, S. Dittmaier, and M. M. Weber. Precise predictions for the Higgs-boson decay $H \rightarrow WW/ZZ \rightarrow 4$ leptons. *Phys. Rev. D*, 74:013004, 2006.
- [30] A. Bredenstein, Ansgar Denner, S. Dittmaier, and M. M. Weber. Precision calculations for the Higgs decays $H \rightarrow ZZ/WW \rightarrow 4$ leptons. *Nucl. Phys. B Proc. Suppl.*, 160:131–135, 2006.
- [31] A. De Rujula, Joseph Lykken, Maurizio Pierini, Christopher Rogan, and Maria Spiropulu. Higgs Look-Alikes at the LHC. *Phys. Rev. D*, 82:013003, 2010.
- [32] Yanyan Gao, Andrei V. Gritsan, Zijin Guo, Kirill Melnikov, Markus Schulze, and Nhan V. Tran. Spin Determination of Single-Produced Resonances at Hadron Colliders. *Phys. Rev. D*, 81:075022, 2010.
- [33] Sara Bolognesi, Yanyan Gao, Andrei V. Gritsan, Kirill Melnikov, Markus Schulze, Nhan V. Tran, and Andrew Whitbeck. On the Spin and Parity of a Single-Produced Resonance at the LHC. *Phys. Rev. D*, 86:095031, 2012.
- [34] Serguei Chatrchyan et al. Study of the Mass and Spin-Parity of the Higgs Boson Candidate Via Its Decays to Z Boson Pairs. *Phys. Rev. Lett.*, 110(8):081803, 2013.
- [35] J R Andersen et al. Handbook of LHC Higgs Cross Sections: 3. Higgs Properties. 7 2013.
- [36] Serguei Chatrchyan et al. Observation of a New Boson with Mass Near 125 GeV in pp Collisions at $\sqrt{s} = 7$ and 8 TeV. *JHEP*, 06:081, 2013.
- [37] Georges Aad et al. Evidence for the spin-0 nature of the Higgs boson using ATLAS data. *Phys. Lett. B*, 726:120–144, 2013.
- [38] Serguei Chatrchyan et al. Measurement of the Properties of a Higgs Boson in the Four-Lepton Final State. *Phys. Rev. D*, 89(9):092007, 2014.
- [39] Suyong Choi, Sunghoon Jung, and P. Ko. Implications of LHC data on 125 GeV Higgs-like boson for the Standard Model and its various extensions. *JHEP*, 10:225, 2013.
- [40] Vardan Khachatryan et al. Constraints on the spin-parity and anomalous HVV couplings of the Higgs boson in proton collisions at 7 and 8 TeV. *Phys. Rev. D*, 92(1):012004, 2015.
- [41] Martin Beneke, Diogo Boito, and Yu-Ming Wang. Anomalous Higgs couplings in angular asymmetries of $H \rightarrow Z\ell^+\ell^-$ and $e^+e^- \rightarrow HZ$. *JHEP*, 11:028, 2014.

- [42] James S. Gainer, Joseph Lykken, Konstantin T. Matchev, Stephen Mrenna, and Myeonghun Park. Beyond Geolocating: Constraining Higher Dimensional Operators in $H \rightarrow 4\ell$ with Off-Shell Production and More. *Phys. Rev. D*, 91(3):035011, 2015.
- [43] Albert M Sirunyan et al. Constraints on anomalous Higgs boson couplings using production and decay information in the four-lepton final state. *Phys. Lett. B*, 775:1–24, 2017.
- [44] Sally Dawson, Christoph Englert, and Tilman Plehn. Higgs Physics: It ain’t over till it’s over. *Phys. Rept.*, 816:1–85, 2019.
- [45] Daniel Stolarski and Roberto Vega-Morales. Directly Measuring the Tensor Structure of the Scalar Coupling to Gauge Bosons. *Phys. Rev. D*, 86:117504, 2012.
- [46] Ian Low, Joseph Lykken, and Gabe Shaughnessy. Have We Observed the Higgs (Imposter)? *Phys. Rev. D*, 86:093012, 2012.
- [47] Tyler Corbett, O. J. P. Eboli, J. Gonzalez-Fraile, and M. C. Gonzalez-Garcia. Constraining anomalous Higgs interactions. *Phys. Rev. D*, 86:075013, 2012.
- [48] Ian Anderson et al. Constraining Anomalous HVV Interactions at Proton and Lepton Colliders. *Phys. Rev. D*, 89(3):035007, 2014.
- [49] John Ellis and Dae Sung Hwang. Does the ‘Higgs’ have Spin Zero? *JHEP*, 09:071, 2012.
- [50] John Ellis, Ricky Fok, Dae Sung Hwang, Veronica Sanz, and Tevong You. Distinguishing ‘Higgs’ spin hypotheses using $\gamma\gamma$ and WW^* decays. *Eur. Phys. J. C*, 73:2488, 2013.
- [51] Alexandre Alves. Is the New Resonance Spin 0 or 2? Taking a Step Forward in the Higgs Boson Discovery. *Phys. Rev. D*, 86:113010, 2012.
- [52] S. Y. Choi, M. M. Muhlleitner, and P. M. Zerwas. Theoretical Basis of Higgs-Spin Analysis in $H \rightarrow \gamma\gamma$ and $Z\gamma$ Decays. *Phys. Lett. B*, 718:1031–1035, 2013.
- [53] Jeffrey Davis, Andrei V. Gritsan, Lucas S. Mandacaru Guerra, Savvas Kyriacou, Jeffrey Roskes, and Markus Schulze. Constraining anomalous Higgs boson couplings to virtual photons. *Phys. Rev. D*, 105(9):096027, 2022.
- [54] A. Soni and R. M. Xu. Probing CP violation via Higgs decays to four leptons. *Phys. Rev. D*, 48:5259–5263, 1993.
- [55] Darwin Chang, Wai-Yee Keung, and Ivan Phillips. CP odd correlation in the decay of neutral Higgs boson into $Z Z$, $W^+ W^-$, or $t \text{ anti-}t$. *Phys. Rev. D*, 48:3225–3234, 1993.
- [56] Rohini M. Godbole, D. J. Miller, and M. Margarete Muhlleitner. Aspects of CP violation in the $H ZZ$ coupling at the LHC. *JHEP*, 12:031, 2007.
- [57] Charles A. Nelson. CP / P Determination and Other Applications of τ Lepton and T Quark Polarimetry. *Phys. Rev. D*, 41:2805, 1990.
- [58] B. Grzadkowski and J. F. Gunion. Using decay angle correlations to detect CP violation in the neutral Higgs sector. *Phys. Lett. B*, 350:218–224, 1995.

- [59] Tilman Plehn, David L. Rainwater, and Dieter Zeppenfeld. Determining the Structure of Higgs Couplings at the LHC. *Phys. Rev. Lett.*, 88:051801, 2002.
- [60] Kaoru Hagiwara, Qiang Li, and Kentarou Mawatari. Jet angular correlation in vector-boson fusion processes at hadron colliders. *JHEP*, 07:101, 2009.
- [61] Christoph Englert, Dorival Goncalves-Netto, Kentarou Mawatari, and Tilman Plehn. Higgs Quantum Numbers in Weak Boson Fusion. *JHEP*, 01:148, 2013.
- [62] Vernon D. Barger, King-man Cheung, A. Djouadi, Bernd A. Kniehl, and P. M. Zerwas. Higgs bosons: Intermediate mass range at e^+e^- colliders. *Phys. Rev. D*, 49:79–90, 1994.
- [63] D. J. Miller, S. Y. Choi, B. Eberle, M. M. Muhlleitner, and P. M. Zerwas. Measuring the spin of the Higgs boson. *Phys. Lett. B*, 505:149–154, 2001.
- [64] John Ellis, Verónica Sanz, and Tevong You. Associated Production Evidence against Higgs Impostors and Anomalous Couplings. *Eur. Phys. J. C*, 73:2507, 2013.
- [65] P. Artoisenet et al. A framework for Higgs characterisation. *JHEP*, 11:043, 2013.
- [66] Kumar Rao and Saurabh D. Rindani. Probing CP-violating contact interactions in $e^+e^- \rightarrow HZ$ with polarized beams. *Phys. Lett. B*, 642:85–92, 2006.
- [67] Kumar Rao and Saurabh D. Rindani. Charged lepton distributions as a probe of contact e^+e^-HZ interactions at a linear collider with polarized beams. *Phys. Rev. D*, 77:015009, 2008. [Erratum: *Phys.Rev.D* 80, 019901 (2009)].
- [68] Katri Huitu, Kumar Rao, Saurabh D. Rindani, and Pankaj Sharma. Effective fermion-Higgs interactions at an e^+e^- collider with polarized beams. *Nucl. Phys. B*, 911:274–294, 2016.
- [69] Benjamín Grinstein, Christopher W. Murphy, and David Pirtskhalava. Searching for New Physics in the Three-Body Decays of the Higgs-like Particle. *JHEP*, 10:077, 2013.
- [70] Andrei V. Gritsan, Jeffrey Roskes, Ulascan Sarica, Markus Schulze, Meng Xiao, and Yaofu Zhou. New features in the JHU generator framework: constraining Higgs boson properties from on-shell and off-shell production. *Phys. Rev. D*, 102(5):056022, 2020.
- [71] Seong Youl Choi and Jae Hoon Jeong. Selection rules for the decay of a particle into two identical massless particles of any spin. *Phys. Rev. D*, 103(9):096013, 2021.
- [72] Seong Youl Choi and Jae Hoon Jeong. Weaving the covariant three-point vertices efficiently. *Phys. Rev. D*, 104(5):055046, 2021.
- [73] Seong Youl Choi and Jae Hoon Jeong. Constructing the covariant three-point vertices systematically. *Phys. Rev. D*, 105(1):016016, 2022.
- [74] A. Djouadi, J. Kalinowski, and M. Spira. HDECAY: A Program for Higgs boson decays in the standard model and its supersymmetric extension. *Comput. Phys. Commun.*, 108:56–74, 1998.
- [75] Abdelhak Djouadi, Jan Kalinowski, Margarete Muehlleitner, and Michael Spira. HDECAY: Twenty₊₊ years after. *Comput. Phys. Commun.*, 238:214–231, 2019.

- [76] R. E. Behrends and C. Fronsdal. Fermi Decay of Higher Spin Particles. *Phys. Rev.*, 106(2):345, 1957.
- [77] P. R. Auvil and J. J. Brehm. Wave Functions for Particles of Higher Spin. *Phys. Rev.*, 145(4):1152, 1966.
- [78] P. J. Caudrey, I. J. Ketley, and R. C. King. Covariant arbitrary-spin wave functions and helicity couplings. *Nucl. Phys. B*, 6:671–686, 1968.
- [79] Michael D. Scadron. Covariant Propagators and Vertex Functions for Any Spin. *Phys. Rev.*, 165:1640–1647, 1968.
- [80] S. U. Chung. A General formulation of covariant helicity coupling amplitudes. *Phys. Rev. D*, 57:431–442, 1998.
- [81] Shi-Zhong Huang, Tu-Nan Ruan, Ning Wu, and Zhi-Peng Zheng. Solution to the Rarita-Schwinger equations. *Eur. Phys. J. C*, 26:609–623, 2003.
- [82] G. C. Wick. Angular momentum states for three relativistic particles. *Annals Phys.*, 18:65–80, 1962.
- [83] Herbi K. Dreiner, Howard E. Haber, and Stephen P. Martin. Two-component spinor techniques and Feynman rules for quantum field theory and supersymmetry. *Phys. Rept.*, 494:1–196, 2010.
- [84] Herbi K. Dreiner, Howard E. Haber, and Stephen P. Martin. *From Spinors to Supersymmetry*. Cambridge University Press, Cambridge, UK, 7 2023.
- [85] A. D. Martin and T. D. Spearman. *Elementary Particle Theory*. North-Holland Publishing Co., Amsterdam, 1970.
- [86] Elliot Leader. *Spin in Particle Physics*, volume 15 of *Cambridge Monographs on Particle Physics, Nuclear Physics and Cosmology*. Cambridge University Press, 7 2023.
- [87] Seong Youl Choi, Jae Hoon Jeong, and Ji Ho Song. General Spin Analysis from Angular Correlations in Two-Body Decays. *Eur. Phys. J. Plus*, 135(2):210, 2020.
- [88] M. Jacob and G. C. Wick. On the General Theory of Collisions for Particles with Spin. *Annals Phys.*, 7:404–428, 1959.
- [89] M.E. Rose. *Elementary Theory of Angular Momentum*. Dover Books on Physics Series. Dover Publications, Incorporated, 2013.
- [90] S. Mandelstam. Determination of the pion - nucleon scattering amplitude from dispersion relations and unitarity. General theory. *Phys. Rev.*, 112:1344–1360, 1958.
- [91] Wai-Yee Keung and William J. Marciano. HIGGS SCALAR DECAYS: $H \rightarrow W^+ X$. *Phys. Rev. D*, 30:248, 1984.
- [92] Marc Hohlfeld. On the determination of Higgs parameters in the ATLAS experiment at the LHC. 8 2000.

- [93] M. Kramer, Johann H. Kuhn, M. L. Stong, and P. M. Zerwas. Prospects of measuring the parity of Higgs particles. *Z. Phys. C*, 64:21–30, 1994.
- [94] Kaoru Hagiwara and M. L. Stong. Probing the scalar sector in $e^+ e^- \rightarrow f \text{ anti-}f$ H. *Z. Phys. C*, 62:99–108, 1994.
- [95] Kaoru Hagiwara, S. Ishihara, J. Kamoshita, and Bernd A. Kniehl. Prospects of measuring general Higgs couplings at $e^+ e^-$ linear colliders. *Eur. Phys. J. C*, 14:457–468, 2000.
- [96] Bohdan Grzadkowski, John F. Gunion, and Jacek Pliszka. How valuable is polarization at a muon collider? A Test case: Determining the CP nature of a Higgs boson. *Nucl. Phys. B*, 583:49–75, 2000.
- [97] Tao Han and J. Jiang. CP violating $Z Z H$ coupling at $e^+ e^-$ linear colliders. *Phys. Rev. D*, 63:096007, 2001.
- [98] Nima Arkani-Hamed, Savvas Dimopoulos, and G. R. Dvali. The Hierarchy problem and new dimensions at a millimeter. *Phys. Lett. B*, 429:263–272, 1998.
- [99] Ignatios Antoniadis, Nima Arkani-Hamed, Savvas Dimopoulos, and G. R. Dvali. New dimensions at a millimeter to a Fermi and superstrings at a TeV. *Phys. Lett. B*, 436:257–263, 1998.
- [100] Tao Han, Joseph D. Lykken, and Ren-Jie Zhang. On Kaluza-Klein states from large extra dimensions. *Phys. Rev. D*, 59:105006, 1999.
- [101] Albert M Sirunyan et al. Measurements of production cross sections of the Higgs boson in the four-lepton final state in proton–proton collisions at $\sqrt{s} = 13$ TeV. *Eur. Phys. J. C*, 81(6):488, 2021.
- [102] L. D. Landau. On the angular momentum of a system of two photons. *Dokl. Akad. Nauk SSSR*, 60(2):207–209, 1948.
- [103] Chen-Ning Yang. Selection Rules for the Dematerialization of a Particle Into Two Photons. *Phys. Rev.*, 77:242–245, 1950.
- [104] Vardan Khachatryan et al. Observation of the Diphoton Decay of the Higgs Boson and Measurement of Its Properties. *Eur. Phys. J. C*, 74(10):3076, 2014.
- [105] John M. Cornwall, David N. Levin, and George Tiktopoulos. Uniqueness of spontaneously broken gauge theories. *Phys. Rev. Lett.*, 30:1268–1270, 1973. [Erratum: *Phys.Rev.Lett.* 31, 572 (1973)].
- [106] John M. Cornwall, David N. Levin, and George Tiktopoulos. Derivation of Gauge Invariance from High-Energy Unitarity Bounds on the s Matrix. *Phys. Rev. D*, 10:1145, 1974. [Erratum: *Phys.Rev.D* 11, 972 (1975)].
- [107] C. H. Llewellyn Smith. High-Energy Behavior and Gauge Symmetry. *Phys. Lett. B*, 46:233–236, 1973.

- [108] Benjamin W. Lee, C. Quigg, and H. B. Thacker. The Strength of Weak Interactions at Very High-Energies and the Higgs Boson Mass. *Phys. Rev. Lett.*, 38:883–885, 1977.
- [109] Benjamin W. Lee, C. Quigg, and H. B. Thacker. Weak Interactions at Very High-Energies: The Role of the Higgs Boson Mass. *Phys. Rev. D*, 16:1519, 1977.
- [110] L. Rossi and O. Brüning. Introduction to the HL-LHC Project. *Adv. Ser. Direct. High Energy Phys.*, 24:1–17, 2015.